CZECH TECHNICAL UNIVERSITY IN PRAGUE

FACULTY OF BIOMEDICAL ENGINEERING

Department of Biomedical Technology

Cyclodextrin-Based Nanogel Delivery Platform for Hydrophobic Drug Delivery

Master thesis

Study programme: Biomedical and Clinical Engineering - CEMACUBE

Author of the master thesis: Justin Jehan Du Maurier Malherbe – BSC Chemical Engineering

Supervisor of the master thesis: Dr. Patrick van Rijn

Associate Professor (UHD), Biomedical Engineering, UMCG

Daily supervisor of the master thesis: Yanjin Ji - B.Sc. & M.Sc. in Stomatology

Mentor: Prof. Bart Verkerke

Dept. of Rehabilitation Medicine, Center for Rehabilitation

Kladno, September 2022

MASTER'S THESIS ASSIGNMENT

I. PERSONAL AND STUDY DETAILS

Student's name:	**Malherbe Justin Jehan Du Maur**	Personal ID number:	**499492**
Faculty:	**Faculty of Biomedical Engineering**		
Department:	**Department of Biomedical Technology**		
Study program:	**Biomedical and Clinical Engineering**		

II. MASTER'S THESIS DETAILS

Master's thesis title in English:

Cyclodextrin-based nanogel delivery platform for hydrophobic drug delivery

Master's thesis title in Czech:

Nanogelová platforma pro podávání hydrofobních léčiv na bázi cyklodextrinů

Guidelines:

Due to their hydrophobic properties, nanogels are a highly promising nanocarrier for the transport or delivery of specific drugs with synergetic behaviour between nanogels and potential biological applications for targeted treatment of acute and chronic diseases. Propose and test a nanogel based on N-isopropylmethacrylamide and B-Cylcodextrin for protected transport of hydrophobic drugs through precipitation polymerisation. Functionalise B-Cylcodextrin as a comonomer, synthesise a novel functional cyclodextrin-based nanogel, and characterise the nanogel and the efficiency of functionalisation. Characterise the nanogel through dynamic light scattering, nuclear magnetic resonance and Fourier transform infrared spectroscopies as well as scanning electron microscopy and transmission electron microscopy if needed. Discuss the results for potential use as a hydrophobic drug vector in future treatments.

Bibliography / sources:

[1] Mauri, E.,Giannitelli, S. M., Trombetta, M., Rainer, A., Synthesis of Nanogels: Current Trends and Future Outlook, Gels, ročník 7, číslo 2, 2021, https:// doi.org/10.3390/gels7020036
[2] Gadade, D. D., Pekamwar, S. S., Cyclodextrin Based Nanoparticles for Drug Delivery and Theranostics, Advanced Pharmaceutical Bulletin, ročník 10, číslo 2, 2020, 166-183 s., https://apb.tbzmed.ac.ir/Article/apb-27565
[3] Zu, G., Mergel, O., Ribovski, L., Bron, R., Zuhorn, I., van Rijn, P., Nanogels with Selective Intracellular Reactivity for Intracellular Tracking and Delivery, Chemistry, ročník 26, číslo 66, 2020, https://doi.org/10.1002/chem.202001802
[4] Keskin, D., Zu, G., Forson, A. M., Tromp, L., Sjollema, J., van Rijn, P., Nanogels: A novel approach in antimicrobial delivery systems and antimicrobial coatings, Bioactive Materials, ročník 6, číslo 10, 2021, doi:10.1016/j.bioactmat.2021.03.004

Name of master's thesis supervisor:

Ing. Jakub Ráfl, Ph.D.

Name of master's thesis consultant:

Dr. Patrick Van Rijn, Associate Professor, University of Groningen

Date of master's thesis assignment: **02.03.2022**
Assignment valid until: **30.09.2023**

doc. Ing. Martin Rožánek, Ph.D.	prof. MUDr. Jozef Rosina, Ph.D., MBA
Head of department	Dean

DECLARATION

I hereby declare that I have completed this thesis with the topic "**Cyclodextrin-based Nanogel Delivery Platform for Hydrophobic Drug Delivery**" independently, and that I have attached an exhaustive list of citations of the employed sources.

I do not have a compelling reason against the use of the thesis within the meaning of Section 60 of Act No. 121/2000 Sb., on copyright, rights related to copyright, and amending some laws (Copyright Act).

In Kladno 08 August 2022

Justin Jehan Du Maurier Malherbe, BSc. Chemical Engineering

'Science means constantly walking a tightrope between blind faith and curiosity; between expertise and creativity; between bias and openness; between experience and epiphany; between ambition and passion and between arrogance and conviction - in short, between an old today and a new tomorrow.'

Heinrich Rohrer

ACKNOWLEDGEMENTS

I would like to thank my supervisor, Dr. Patrick van Rijn, for his guidance and support in generating this opportunity, filling in extra supervision roles, and refining the goals as progress was made. The BME department at UMCG has the opportunity to be part of a constructive and supportive team and work environment with the Biomaterials Science group in the BME department at Groningen. I would like to thank Yanjing Ji as my daily supervisor for support in concurrent experiments and assistance in spectral analysis. I also thank Dr. Damla Keskin for briefly providing guidance in her last month as a postdoctoral researcher. Thank you to all those who are in Patrick's group and the welcoming environment of the BME department, the barbecues and the social balance provided outside of the thesis obligations.

A special thanks goes to Dr. Aldona Mzyk for her guidance and critical analysis of experiments, writing, and general management of the investigation and reintroduction into the academic environment. To Irem Soyhan for her contributions in nanoparticles to this thesis as an alternative comparison and for discussions on nanoparticles and synergetic brainstorming sessions with her and Adi Mohan on common characterisation techniques. A thank you Bryn David Monnery for his assistance and guidance on polymer and chemical techniques within the lab. To Prof. Bart Verkerke, my mentor, for helping in situations of strife and his general guidance in difficult times regarding moving countries and maintaining the program and thesis. To Irma Knevel for continuously encouraging and supporting the CEMACUBE group to extraordinary lengths as her final cohort. To Jacopo Poppi, Jonah Renting, Laurens Bosscher Navarro, and Adi Mohan for the incredible working environment and balance created in the MSc office and throughout each week while working at UMCG and completing the investigation.

Lastly, but not least, I would like to sincerely thank my family. To my father and mother for the sacrifices made to make this opportunity possible, for the encouragement, support, and belief in pursuing this goal no matter the hurdles. To my brother, for always having my back without question. May you all share in this success with me as if it were your own.

Master Thesis Title:

Cyclodextrin-based Nanogel Delivery Platform for Hydrophobic Drug Delivery

Abstract:

A key problem in healthcare is the predominance of bacterial infections, resistance development through environmental build-up. While novel antimicrobials have been developed, there is a need for nanoscale drug vectors for these agents. The investigation aimed to create a novel cyclodextrin based nanogel for the primary purpose of encapsulating a photosensitive azobenzene-based antimicrobial drug. This drug has ability to self-regulate deactivation within the body, mitigating concerns of antimicrobial build-up and associated resistance. A coprecipitation polymerisation method was to combine N-isopropylmethacrylamide and a functionalized derivative of a β-CD.

Issues were encountered with characterisation techniques and loading of azobenzene. The loading capacity was found to be equivalent to the atypical binding capacity through UV/VIS spectroscopy. However, it was inconclusive as to whether cyclodextrin had been successfully incorporated and a novel nanogel had been successfully synthesised.

An alternative synthesis method was employed using NIPAM which showed successful inclusion. This nanogel complex was synthesised using an EDC/NHS crosslinking based approach. Additionally, further investigation of cyclodextrin nanogels of varied molar equivalence would be needed to verify the success. Along with Nile Red, repeated FTIR and additional loading experiments could evaluate the potential success of co-polymerisation. Both techniques could then be further tested for loading capacity and triggered release and their characteristic capacity and behaviour compared.

Keywords:

Nanogel, Antimicrobial Resistance, Azobenzene, β-Cyclodextrin, Drug Delivery

Table of Contents

List of symbols and abbreviations 7
1 Introduction 8
1.1 Motivation and background 8
1.2 Overview of the current state of the art 11
1.2.1 Nanoparticles in Nanomedicine and Biomedical Engineering 11
1.2.2 Technique and Polymer Selection and Characteristic Behaviour 13
1.2.3 Cyclodextrin – The hydrophobic pocket 17
1.3 Aims of thesis 21
2 Materials & Methods 22
2.1 Materials 22
2.2 Methods 23
2.2.1 Graphical Overview of Systematic Approach 23
2.2.2 Preparation of β-Cyclodextrin for Co-polymerisation 24
2.2.3 Syntheses by Precipitation Polymerization 30
2.2.4 Characterisation, Verification and Drug Modelling 33
3 Results 37
3.1 Average size, Zeta potential and VPTT of NIPMAM and CD Nanogels from DLS 37
3.1.1 Average Size and Zeta Potential 37
3.1.2 VPTT measurements for NIPMAM and CD-*co*-NIPMAM NG's 39
3.2 Primary characterisation from HNMR 41
3.3 Secondary characterisation by FTIR 42
3.4 UV/VIS 45
3.4.1 Standard Curves and Loading Capacity 45
3.4.2 AZ Triggered release with Irradiation 47
4 Discussion 48
4.1 DLS/Zeta and VPTT Measurements 48
4.2 HNMR and FTIR – 1st and 2nd Characterisation 50
4.3 UV/VIS AZ atypical binding and loading 52
4.4 Clinical Relevance, Limitations and Recommendations 54
5 Conclusions 58
6 Ethics Paragraph 60
List of Literature 62
List of Appendices 65

List of symbols and abbreviations

- **Nanogels (NG's)**
- **Volume Phase Transition Temperature (VPTT)**
- **Lower Critical Solution Temperature (LCST)**
- **Room Temperature (RT)**
- **Dynamic Light Scattering (DLS)**
- **Ultraviolet/Visible Light (UV/VIS)**
- **Fourier Transformed Infrared Spectroscopy (FTIR)**
- **Hydrogen Nuclear Magnetic Resonance Spectroscopy (HNMR)**
- **Signal-to-noise ratio (S/N)**
- **Blood Brain Barrier (BBB)**
- **Cyclodextrin and NIPMAM copolymerized nanogel (CD-*co*-NIPMAM NG)**
- **NIPMAM nanogel copolymerised with AACD P(NIPMAM)-co-AACD**
- **Three-dimensional (3D)**
- **Glioblastoma Multiforme (GBM)**
- **Heptakis- (6-amino-6deoxy)-B-Cylcodextrin heptachloride (Ha-β-CD)**
- **Precipitation polymerisation (PP)**
- **Cyclodextrin (CD)**
- **Beta-Cyclodextrin (β-CD)**
- **N-isopropylmethacrylamide (NIPMAM)**
- **Acrylic Acid (AA)**
- **Acrylate-functionalized Cyclodextrin (AA-CD)**
- **Heptakis-β-Cyclodextrin (Ha-β-CD)**
- **Hydroxyl (OH)**
- **Azobenzene (AZ)**
- **1-ethyl-3-[3-dimethylaminopropyl]carbodiimide hydrochloride (EDC)**
- **(N-[3(Dimethylamino)propyl]methacrylamide (DMAPMA)**
- **N-Hydroxysuccinimide (NHS)**
- **4-Morpholineethanesulfonic acid (MES)**
- **methoxy azobenzene (MeO-AZ)**

1 Introduction

1.1 Motivation and background

A ubiquitous problem in healthcare is the predominance of bacterial infections and their leading cause of mortality, chronic infections, infectious diseases, health risks in biomedical fields and interventions, textile and food industries, marine equipment and ecosystems, as well as water sanitations and purification systems ([12,16,31]).

Infectious diseases are caused by pathogenic microbes such as bacteria, viruses, fungi, and parasites. These have significant and diverse adverse effects on the human condition and health, as well as creating abundant tolls on public health care systems and economies, especially those in developing countries ([10,24]). Many of these infectious diseases have caused the deaths of millions of people around the world every year ([24]). The preferential mechanism of treatment to stem the tide of infectious diseases, especially bacterial infections, is the use of antibiotics ([31]). These are crucial for the success of modern medicine and the facilitation of successful surgical operations([24,29,33]). Their use stems from their inherent cost-effectiveness and powerful results ([31]).

Various antimicrobials agents have been produced naturally, synthetically, or through chemical modification to inhibit the growth of various pathogenic microorganisms such as bacteria, fungi, and viruses ([7]). In some cases, throughout their use of these antimicrobial agents or antibiotics have resulted in desirable lethal effects against various bacterial infections ([7]).

However, a plethora of infections and illnesses have surfaced due to misuse, irregular implementation, and overuse leading to significant a health crisis in the modern world relating to antibiotic and even multidrug-resistant organisms (MDROs) ([16]). Furthermore, some studies have shown super bacteria resistant to nearly all antibiotic variants ([31]). This creates an ever increasing economic and time-consuming investment [16] to develop alternatives, as current administration regimes would use high antibiotic doses. This compounds the already challenging build-up of antibiotics in the environment, adversely affecting the emergence and proliferation of mutations and resistance development ([7,16,29,31]).

Even with significant investment into awareness campaigns and programmes to counteract misuse and overuse of antibiotics in a range of human, agriculture, and animal industries, there is an urgent need for innovative solutions to mitigate the selective evolutionary pressure on bacteria due to antibiotic build-ups ([29]). As a result, one of the key areas of focus is the development of novel molecular solutions that address the administration of antimicrobial agents without facilitating the build-up of these antibiotics in the environment ([29]).

An emerging solution in pharmacology and photochemotherapy has shown promise in dealing with systemic and environmental adverse effects of chemotherapy and antimicrobial treatments ([33]). The inclusion of molecular photo switches that allow remote antimicrobial control through light-induced bioactivity shows significant potential as a molecular solution ([29,33]).

Light regulation has gained traction as a triggered control for biological activity as it is a relatively non-invasive technique, has attractive resolution capabilities, and limited contamination potential while maintaining a high degree of control over intensity and wavelength in application ([29]). Furthermore, light in principle is not harmful and is delivered with high precision and has found application in antibacterial photodynamic therapies ([25,29]). Phototherapies have seen clinical application in control of neuronal networks, vision restoration, antitumor therapy and of particular focus in this investigation, the use of photo switchable antimicrobials ([33]).

When irradiated with light of specific wavelengths, photo-switching enantiomer molecules undergo reversable changes in their structure, and therefore their properties and biological activity. This conformational shift makes these photo isomers biologically effective in one configuration and ineffective in another allowing precise treatment, effectiveness and deactivation control ([25,29]). Photo-pharmacology has shown successful application of these techniques in photo-control of enzyme activity, receptor affinity, motility of an entire organism or of specific interest in this investigation the refined control of antimicrobial activity ([29]).

Of particular interest is the inclusion of innate auto-deactivation ability in the antibacterial agents and biocompounds to directly mitigate concerns of antibiotic accumulation in the environment. In recent years, at the University of Groningen, ([29]),

photo-switching and auto-deactivating antimicrobial agents have been developed using a frequently used photo-actuator enantiomer, Azobenzene (AZ) with designs based on quinolones and precursors toward tryptophan synthase ([25,29]). Investigations have been published by authors Michael Wegener, Willem A. Velema, Nadja A. Simeth ([25,29,33]).

When irradiated with light of a specific wavelength the E isomer (Trans), which is thermodynamically more stable and strongly bound, is converted to its Z conformation (CIS) ([25]). The Z conformation change causes a change in its UV/VIS absorption spectrum, polarity and an increase in steric demand and in some cases its affinity towards enzymes. In its Z conformation the AZ based compound is not only weakly bound to its host complex and released but this shift causes the activation of its antimicrobial state in the quinolone designs. This change can be reversed with irradiation of a light with lower energy or thermally ([25]). It has been shown that the quinolone design, which will be the focus of this investigation, would see thermal auto-deactivation in the human body over the span of only a few hours ([29]). This design provides an innovative solution to a growing global health problem while mitigating antibiotic build-up concerns. Then, attention is drawn to the vector that will be used to deliver this innovative antibiotic.

The current investigation explores the idea of creating a novel nanoscale hydrophobic drug delivery platform for this photo-actuation-based antimicrobial drug, allowing for triggered release by irradiation with light. The emphasis is placed on using the known synergetic effects of co-polymerised nanoparticles as drug delivery platforms for antimicrobials ([7]), the clinical relevance of the specific synthesis technique employed, precipitation polymerisation, and the synergetic effects applicable polymers, cyclodextrin (CD) and NIPMAM/NIPAM. These explorations lead to the proposed aim of creating a nanogel hydrophobic drug delivery platform designed on a combination of CD and a thermoresponsive polymer. The proposed synthesis technique chosen for investigation was precipitation polymerisation. These concepts are detailed in the subsequent state-of-the-art sections before attention is drawn to the specific techniques employed to achieve this goal. Specific detail will be drawn to; state of the art of general nanogels and their proliferation in industry, their applicability as drug vectors, the choices of polymers and synthesis techniques, synergetic capabilities of CD inclusion as well as modifications of CD that may enhance drug delivery capabilities.

1.2 Overview of the current state of the art

1.2.1 Nanoparticles in Nanomedicine and Biomedical Engineering

Nanogels (NGs) have enjoyed significant increase in attention and have shown promise in its suitability for application in biomedical engineering techniques and treatments over the decades ([36–38]). The design of these nanogels facilitates important and specific roles in advanced treatment methods targeting chronic and acute disease, specifically as drug delivery systems. Applications range from treatments for tumours to neurological disorders ([17]). This stems from the atomic and molecular manipulation capabilities of nanogels, allowing for a wide range of application potential. These can come in the form of lipid nanoparticles, liposomes, polymeric nanoparticles and micelles, inorganic nanostructures, or hybrid systems ([34]).

Within these treatment applications NGs have found roles in areas ranging from catalysis, diagnostics, and delivery to antifouling coatings among other areas in the biomedical field. NGs are essentially nano-sized hydrogels that are formed either physically or chemically through cross-linking polymeric chains. 3D porous structures are formed that have a high affinity and water absorption capacity while maintaining their integrity without dissolution in aqueous mediums. Commonly, these are spherically shaped nanoparticles that can be designed to have heterogenous interwoven bulk-like structures or core-shell-like structures although other modulations are viable ([17]).

NG-based treatment inclusions allow for the possibility of easily exchanging active structures ([36]). The susceptibility of NGs to hydrolysis-based decay in intracellular environments and therefore the selective release of their molecular components can be specifically engineered by utilising differences between ester and amide conjugations, as well as chemical modifications ([36]). Using these differences can, in turn, affect the chemical selectivity of NG and result in the controlled release of molecular constituents within the cell, while maintaining no triggered release outside the target cell ([38]). Additionally, compounds such as enantiomeric photo-switching molecules or drugs can be incorporated into the NG's complex ([27,30]). Here, photosensitivity can be used as a drug release mechanism. One three-dimensional (3D) orientation is stable within the

NG complex while the photoinduced mirror image is unstable, causing a controlled release of the compound from the NGs into the surrounding environment ([25,31]).

While many practical advantages have been noted for liposomes and polymerosomes over solid particles, NGs have continuously shown increasing promise as superior alternatives mitigating shortfalls of polymerosomes, liposome, micelles and solid particles. They combine drug loading capacity with adaptability to stability and resilience, emphasising their diverse application potential in biomedical and pharmaceutical interventions ([37,38]).

Of particular interest is the inclusion of covalent polymer networks that provide the stability to cope with environments within the human body. NGs can be programmed through synthesis techniques to respond to specific stimuli in the body, allowing them to undergo high deformations, folding, and reformations without breaking, therefore maintaining specific functions relevant to their intended use ([36–38]).

One characteristic functionality of these NGs is their 'swelling' behaviour. The hydrophilic or water absorption capabilities of the polymers used allow for greater amounts of water, while preserving structural integrity. Molecular interactions allow the solvent molecules to penetrate the nanostructure, elongating the polymer chains until counterbalance forces inhibit further deformation, leading to a 90 w/w % water absorption. This shrinkage and swelling ability improves the diffusion of substances to and from biological structures ([17]). Engineering this behaviour can lead to sensitivity to specific stimulus such as pH, ionic strength, solvent affinity, or temperature ([19]). Within this investigation, the focus will on utilising of thermosensitive polymers in NG synthesis for employment in targeted drug delivery mechanisms.

One of the most pertinent problems nanoscale vectors is addressing is the mortality and health crisis's implications of antimicrobial resistance and build-up in the environment. This has played a key role in the advancement of nanoscale solutions ([29,33]). Although not the direct focus of this investigation, a novel vector would also show promise for another major area of concern in healthcare, mortality due to cancer.

Glioblastomas are one of the most aggressive and difficult cancers to treat. A suggested solution for these hurdles is the use of nanoparticle-based chemotherapy drug

treatments ([1]). This provides an potential alternative technique to those at an impasse due to the blood-brain barrier (BBB), by using blood circulation pathways or pose high dosage complications. Standard treatment methods fail due to the inability to remove all glioblastoma multiforme (GBM) tumor cells ([1]). Inclusion of nanodrugs and nanodrug delivery systems could improve targeting and efficacy of anti-GBM drugs. Key improvements relate to improved BBB diffusion, specific targeting mechanisms, and homogenous drug distribution ([1]). Furthermore, the efficacy of chemotherapy drugs and radiotherapy is improved and the illumination of tumor borders for removal by surgery, among other benefits ([1]).

A recent study at UMCG, Ruhof 2021, investigated TMZ and curcumin loading into quarternised nanogel techniques for glioblastoma treatment. However, hydrolysis of these compounds was not inhibited. This investigation aims to re-address some issues, based on the conclusions of the previously conducted research. The proposed concept is to replace the DMAPMA comonomer with an alternative component capable of encapsulating and protecting hydrophobic drugs. The emphasis is on creating a novel, generalised nanogel vector to be tested on a specific hydrophobic drug recently developed in Groningen ([29]).

1.2.2 Technique and Polymer Selection and Characteristic Behaviour

1.2.2.1 Polymerisation Precipitated Nanoparticles – The Technique

Chemical or physical techniques are used to prepare these polymer nanospheres. Common physical techniques include emulsification, coacervation, and spray drying, which produce wide range size distributions, while the common chemical process is heterogeneous polymerisation. These polymerisation techniques include methods based on suspension, seeded, precipitation, emulsions, and distillation. Most prominently suspension, emulsion, precipitation, and dispersion. Techniques such as spray drying or spray-coating have application potential for implant coatings have been investigated with great success in recent years at UMCG. The method of choice, due to

advantages such as simplicity, is the last of these depicted, Precipitation Polymerisation (PP) depicted in Figure 1.

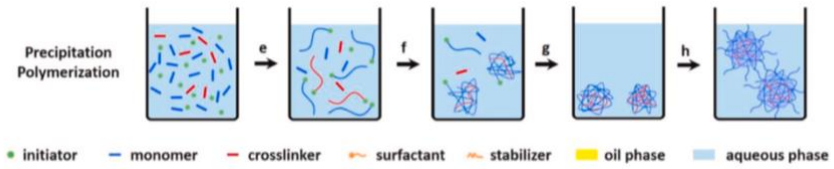

Figure 1 Schematic description of various nanogel formations by heterogenous polymerisation ([12]). The process of heterogenous polymerisation by precipitation shown in the bottom of the figure represents e) initiation, f) precipitation and nucleation by polymer chain collapse above LCST, g) particle growth, and h) transfer to a good solvent or decrease temperature below the VPTT. This is the method that is considered in the investigation and is explained further.

PP, shown in Chemical or physical techniques are used to prepare these polymer nanospheres. Common physical techniques include emulsification, coacervation, and spray drying, which produce wide range size distributions, while the common chemical process is heterogeneous polymerisation. These polymerisation techniques include methods based on suspension, seeded, precipitation, emulsions, and distillation. Most prominently suspension, emulsion, precipitation, and dispersion. Techniques such as spray drying or spray-coating have application potential for implant coatings have been investigated with great success in recent years at UMCG. The method of choice, due to advantages such as simplicity, is the last of these depicted, Precipitation Polymerisation (PP) depicted in Figure 1.

Figure 1 , is a heterogeneous process that begins with a homogeneous system in a continuous phase where monomers, initiators, and colloid stabilisers are dissolved in a solvent. The initiator induces polymerisation of the polymers to form oligomer radicals. When in the presence of cross-linkers these entropically cross-link between oligomer surfaces. As the reaction continues, the capture of oligomers induces growth into microspheres. Above a critical limit, in this case temperature (LCST), this continuous phase becomes a nonsolvent for the polymer microspheres which then precipitate out of solution ([35]). In comparison to emulsion and dispersion methods, precipitation polymerisation has significant advantages. These advantages relate to the absence of a

stabiliser, resulting in a simple and highly efficient protocol for uniform and clean polymer particles with no problems with surfactant removal in the final NG complex. This provides an idyllic simple synthesis technique, involving only monomers, initiators, solvents, cross-linkers, and minimal purification steps ([35]). Moreover, this method differs from methods such as emulsion- and suspension-based techniques which use water-soluble initiators and water-insoluble monomers, processes where the complete removal of the surfactant or stabiliser is very difficult and presents potential complications. In precipitation polymerisation, these are absent from the resulting NG providing ease in purification and separation ([35]).

In short, PP takes place through radical initiation of the monomer and cross-linker homogenous solutions. This is followed by the propagation of chain addition, which results in precipitation of the polymer network in poor solvents below the critical thresholds . This occurs by enthalpic means or entropically when polymer and solvent mixing is prevented by cross-linking. Precipitation polymerisation results in macro or nanoscopic gels, depending on the original monomer concentration. This process results in a narrow size distribution of polymer micro- or nanospheres when there is an absence of a stabiliser or surfactant in the final formation. Characteristic of these nanospheres are the small sizes and volumes, large specific surface areas for light scattering, chemical reactions, and absorption phenomena. Additionally, they have high diffusability and mobility by Brownian motion, stable dispersions due to a balance of steric, electrostatic and van der Waal's forces as well as uniform sized distributions. These traits in addition to the ability to easily vary and fine tune the diameter, surface chemistry, composition, texture, and morphology make these nanoparticles particularly useful in biomedical applications.

1.2.2.2 Polymer Selection

Two specific comonomers were chosen for investigation on the basis of clinical prevalence and potential application for NG drug delivery mechanisms. The primary monomer is an alkylacrylamide, N-Iso-Propyl Methacrylamide (NIMPAM), a thermo-responsive polymer. The secondary monomer is a derivative of oligosaccharide β-Cyclodextrin (β-CD), specifically the chemically modified Heptakis- (6-amino-6deoxy)-B-

Cylcodextrin heptachloride (Ha-B-CD), the reasoning of which is explained in subsequent sections.

The suggested NG's primary constituent is the NIPMAM polymer based on its Lower Critical Solution Temperature (LCST). This is related to its behaviour under physiological conditions and its facilitation of the use of precipitation polymerisation ([36–38]). A similar industry thermosensitive polymer is often used, NIPAM, which varies in structure, as well as LCST and VPTT in precipitation and NG products. For the purposes of this investigation, the alternative NIPMAM was the point of focus. This polymer has a higher LCST and VPTT that is above 37°C, more suitable for biological application. This means that the NG complex would not exhibit shrinking and swelling behaviour in the human body that would be experienced with NIPAM and would remain swollen above 37°C ([6]).

1.2.2.3 Thermosensitive Characteristics and Synthesis Process

NIPMAM and NIPAM exhibit thermosensitive properties and the variation in colloidal behaviour above the LCST in addition to Volume Phase Transition Temperatures (VPTT) based swelling-shrinking behaviour. The thermoresponsive capability of specific nanogels has resulted in a wide adoption for specific use cases biomedical and pharmaceutical applications. The choice of NG constituent is based on the variance in thermal behaviour and, in the case of NIPMAM, its relation to biological reactions in the occurring at 37 ° C. For this reason, the focus is on synthesising a nanogel with NIPMAM as the primary polymer with a LCST of approximately 43-45°C ([6]). However, further functionalisation of the NG complexes or their surfaces through coupling could provide alternatives to the need for LCST based selection such as receptor based characteristic behaviour.

Above this temperature, solubility decreases and dehydration occurs causing collapse and precipitation, micellization and therefore colloid formation. This process is based on a change in solubility above that of the LCST and free radical polymerisation. Resulting colloid formation is due to the most energetically favourable, lowest Gibbs free energy, formation ([37,38]). Energetic favourability causes the collapse of the polymers into spherical particles through micellization, to minimise the unfavourable interactions with the aqueous medium in favour of the energetically favourable structural formation between polymers. Energy minimisation causes the formation of colloid systems,

pushing water out of the micelles to form the most energetically favourable and stable state. This process is based on minimising the interactions of apolar components with the polar surrounding medium. In the collapse, the polar heads are exposed to the polar medium while the hydrophobic apolar components are internalised to reduce the energy of the system. This process can be a "one pot" one step reaction to create a bulk-like NG structure or be repeated, to create a core and shell structure of varied composition ([37,38]).

The characteristic swelling/shrinking behaviour of NGs is the process which is graphically illustrated in in a simple demonstration in **Error! Reference source not found.** using a relevant NIPAM/CD example.

Figure 2 CD-based Hydro/Nanogel Swelling showing characteristic changes above and below LCST/VPTT critical temperatures for a CD-co-NIPAM hydrogel ([32]). The blue cone structures are representative of the included CD cone like cavity structures responsible for hydrophobic drug encapsulation in the nanogel complex.

The degradability, structural integrity, sensitivity to stimulus and responsiveness are specified and manipulated within the synthesis process, therefore, determining the application potential and specificity of the nanogel formed. For the purposes of this investigation the focus will be on the successful synthesis of a bulk-like NG, through precipitation polymerisation comprised of β-CD and NIPMAM or NIPAM.

1.2.3 Cyclodextrin – The hydrophobic pocket

The comonomer selected for synthesis with NIPMAM is β-CD. This synergetic inclusion and choice of comonomer are expanded upon below.

Nanogels are inherently stable without exhibiting disassembly within physiological fluids, providing significant benefits as drug carriers. These advantages pertain to dispersion in aqueous media, passive and active drug targeting and enhanced bioavailability of drugs with the additional ability of triggered drug release when

chemically altered ([18]). However, due to some limitations in drug loading and control of drug release mechanisms, investigations focused on complexes with specific drug affinities obtained through electrostatic, van der Waal and hydrophobic interactions. An area of particular focus centred on the inclusion of CD derivatives into NG complexes. To avoid the collapse of nanogel complexes under high drug loading, phase separation and drug entrapment, a hydrophilic surface becomes an essential characteristic ([18]). Two potential benefits arise from this complex, an affinity-based mechanism for drug loading and release as well as an enhancement of the hydrophilicity of the polymer matrix. These benefits have been demonstrated for macro-hydrogels for sustained drug delivery ([18]).

CD's are a family of macrocyclic oligosaccharides which are composed either of six, seven or eight glucopyranose units with α-glycosidic bonds forming toroidal structures as can be seen in Figure 3**Error! Reference source not found.** below. Of these three variations, β-CD, the comonomer of choice, contains 7 of these functional hydroxyl (OH) units ([14]).

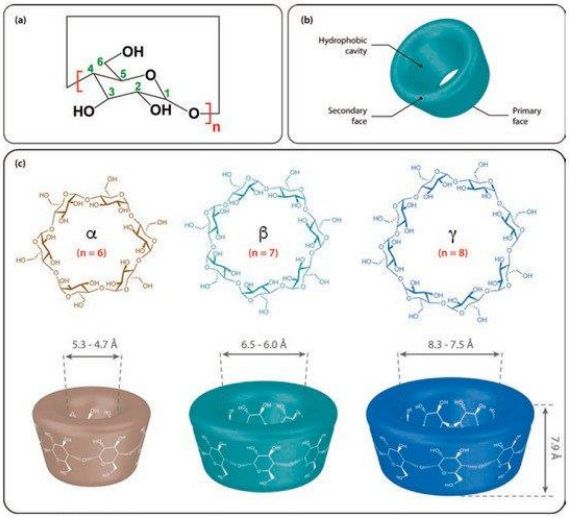

Figure 3 Cyclodextrin structural representations of the monomer unit, overall shape and α, β, γ variants of Cyclodextrin ([15]) COPYRIGHT(2020).

CDs are employed in a variety of pharmaceutical and biomedical applications for chemical and analytical techniques, ranging from purification and spectroscopic analysis to biosensors and fluorescence ([15]). Many of the derivatised versions are used to improve drug bioavailability of pharmaceutical or drug delivery vectors. The core of

these applications is CD's guest-host capability. Encapsulation of a guest molecule achieves several desirable characteristic improvements relating to solubility, stability, volatility, permeability, chemical reactivity or absorption while providing a less toxic composite ([15]). The predominant focus lies in the ability to form selective non-covalent host-guest complexes with small molecules or enantiomeric molecules, through molecular and chiral recognition. The molecular driving forces governing the interaction between CD and guest molecules are electrostatic, van der Waal, hydrophobic interactions and hydrogen bonding. Additionally, this fulfils a need to relieve the conformational strain and high energy ([15]). The interior and exterior properties of the cone-like cavity are due to the C3 and C5 hydrogen and a glycosidic oxygen atom respectively. This results in a desirable hydrophobic interior cavity, with an exterior face that is hydrophilic in nature ([15]).

The exterior hydrophilicity is created by the hydroxyl groups on the face of the cavity which provides hydrophilic interactions with the surrounding hydrophilic components. This creates a water-soluble complex from the hydrophobic drug as well as the aqueous solubility of the compounds ([18]).

The crux of this investigation, is to produce a β-CD-NG complex to encapsulate hydrophobic drugs through hydrophobic interaction. The "water free", hydrophobic pocket of a CD based NG could prove to provide adequate spontaneous encapsulation for a variety of hydrophobic drugs as well as hydrolysis prohibited transport for other targeted pharmaceutical and biomedical treatments, specifically by blood circulation. However, the design is specifically geared towards encapsulating the AZ antimicrobial drug developed at the University of Groningen. This antimicrobial drug comprises of an enantiomeric photosensitive hydrophobic compound, AZ.

AZ undergoes structural changes during light irradiation that have effects on its size, shape, dipole moment, and thermostability, and thus on its interaction with guest-host complexes. The TRANS variant has a zero-dipole moment and a planar configuration, while the CIS conformation has a 3.1 D dipole moment and a configuration opposite to the TRANS variant. The dipole moment affects the hydrophobic/hydrophilic character of the isomers and affects their interaction and binding in guest-host complexes([30]). In this case, the TRANS isomer, characterised by a planar nonpolar structure, would form

strong hydrophobic bonds with the CD cavity interior, whereas the hydrophilic polar CIS isomer would be weakly bound and released when the conformational change is induced. This is the mechanism of interaction used for the encapsulation and release of AZ from the CD complex, which has been investigated in previous studies on the topic ([27]). Illustrations of the conformations can be found in the List of Appendices, page 71.

For the purposes of this investigation, AZ is used as the relevant model hydrophobic drug to investigate the potential encapsulation of the AZ integrated quinolone mentioned previously.

1.2.3.1 β-CD Synergy and comonomer preparation

β-CD containing nanogels presented increased thermosensitivity compared to those without β-CD complexes ([34]). The hydrophobic cavity and the hydrophilic exterior structure promotes and enhances permeability in intestinal mucosa which amplifies the solubility of pharmaceutical drugs. Furthermore, this structure and its amphiphilicity improves the thermally induced swelling behaviour of β-CD-co-NIPMAM hydrogels. However, this has not been widely reported at the nanoparticle level ([34]). For this reason, this investigation focuses on addressing the development of a nanoparticle scale complex of CD and NIPMAM and its potential application in the targeted delivery of hydrophobic drugs, a key objective.

CD rings and their derivatives, such as the chosen β-CD variant can have their ring structure and functional group chemically modified, substituted or linked with substituents or other CD rings to provide building blocks for larger nanostructures or complexes ([9]). This is possible while maintaining their inclusion complex capabilities for hydrophobic molecules. This type of application and functionalisation of CD's is continuously increasing and has demonstrated beneficial impacts especially on biological barriers and at a cellular level ([9]). To utilise β-CD as a co-monomer in the polymerisation precipitation reaction the functional groups need to be chemically modified to acrylate groups.

A key concern in the development of CD based conjugates is the harmful reagents use such as crosslinker species as a result there is a focus on the use of non-toxic reagents

for coupling of carboxylates and generation of primary amide bonds, one such reagent is 1-ethyl-3-[3-dimethylaminopropyl] carbodiimide hydrochloride (EDC) ([13]).

EDC should initially react with the carboxyl groups of β-CD to create an amine reactive *O*-acylisourea intermediate which then forms the needed amide bond by reacting with the primary amine, coupling the β-CD and AA by substituting the NH_2 groups for acrylate functional groups ([13]). However, when NHS is used in combination with EDC the EDC will first couple to NHS carboxylate moieties to form a more stable NHS ester which in turn promotes more efficient coupling reactions. This method does not allow for cross-linking moiety in the product and therefore has a higher biological safety over alternatives ([13]).

1.3 Aims of thesis

The aim of the research was to synthesise a novel CD-based nanogel delivery platform for hydrophobic drug. The focus of the investigation was to create this novel nanogel for the primary purpose of encapsulating a photosensitive enantiomer based antimicrobial drug. An antimicrobial with significant clinical potential and the ability to self-regulate deactivation within the body, mitigating concerns of antimicrobial build-up and associated resistance.

The focal point for this aim was to utilise a simple and clinically relevant co-precipitation polymerisation technique to create this nanogel. The technique aimed to use thermoresponsive polymers, NIPMAM or NIPAM, and a functionalized derivative of β-CD. A CD derivative known to have synergetic properties with various nanoscale drug delivery vectors and applications.

To achieve this, the investigation aimed to first successfully employ partial or full acrylate functionalisation of a β-CD derivative for preparation as a co-monomer in precipitation polymerisation. As such, acrylated CD was then characterised for validation of functionalisation success and efficiency and investigated as the hydrophobic molecular compartment within the nanogel complex in which the drug was loaded.
AZ was used as the hydrophobic drug model for the purposes of atypical binding and loading tests. These tests served validation for its inclusion and its suitability as a hydrophobic drug vector.

An extension of this aim was to contribute to generalised hydrophobic drug and antimicrobial delivery mechanisms. Furthermore, contribute to the generalised fields of photo-pharmacology and chemotherapy-based interventions in the biomedical engineering field.

2 Materials & Methods

2.1 Materials

N-isopropylmethacrylamide (97%, NIPMAM, #423548), N, N' methylenebis (acrylamide) (99%, BIS, #146072), *N*-Isopropylacrylamide (97%, NIPAM), #415324) ammonium persulfate (98%, APS, #A3679), sodium dodecyl sulfate (SDS, #436143) and β-Cyclodextrin (97%, β-CD, #C4767) these were purchased from Sigma-Aldrich, Netherlands. Cellulose dialysis tubes with 1, 2, 6-8 kDa and 12-16 kDa cutoffs were obtained from SpectrumTM, The Netherlands. Heptakis-(6-amino-6-deoxy)-beta-Cyclodextrin heptahydrochloride (>97%, Ha-β-CD, #CY-2065) and 6-Monoamino-6-monodeoxy-beta-Cyclodextrin hydrochloride (>98%, #M2314) were purchased from Cyclodextrin-shop. N-(3-Dimethylaminopropyl)-N'-ethylcarbodiimide hydrochloride (EDC) (>98%, #161462). Acrylic acid N-hydroxysuccinimide ester (≥90%, N-Acryloxysuccinimide, AA-NHS, #A8060), was purchased from Sigma-Aldrich, Netherlands. N-Hydroxysuccinimide (NHS, 98%, # 130672), Hydrochloric acid (ACS reagent, 37%, #320331) and Sodium hydroxide (NaOH, #S8045), 4-Morpholineethanesulfonic acid (MES, M3671), Acrylic acid (#147230) were purchased from Sigma Aldrich, the Netherlands. Nile Red, EtOH, Azobenzene, $NaHCO_3$ and Na_2CO_3 were provided by UMCG, Netherlands. MiliQ was obtained from Milli-Q® Direct Water Purification System. A completed NIPAM NG named AA-NIPAM NG was used that originated from an investigated conducted by Irem Soyhan within the research group at the same time as this thesis.

2.2 Methods

2.2.1 Graphical Overview of Systematic Approach

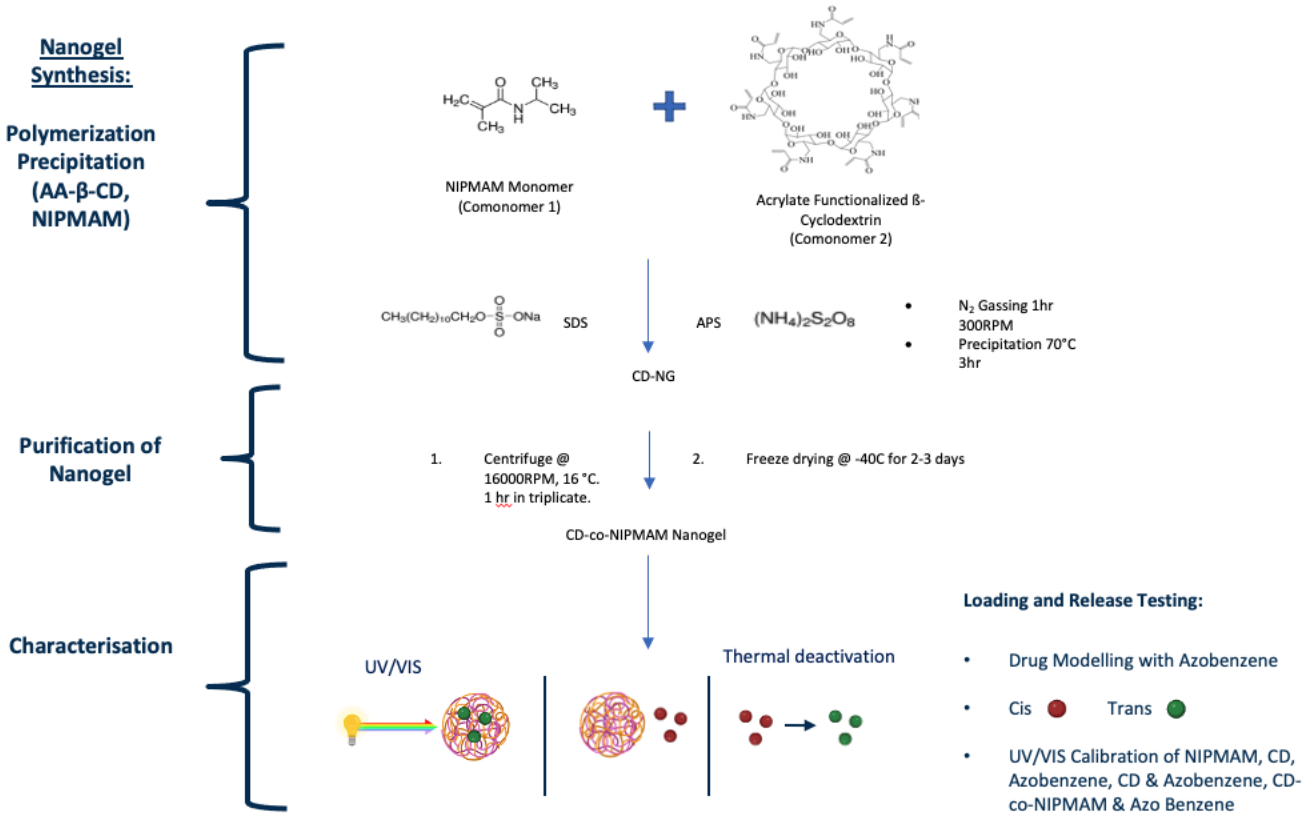

Figure 4 Graphical Illustration of overall investigation process. Images were sources from Sigma Aldrich or created in ChemDraw. Created with BioRender.com.

The overall method starts with the preparation of β-CD as a co-monomer for polymerisation precipitation with NIPMAM, this is achieved by acrylate functionalisation of β-CD to form acrylate functionalised CD (AA-CD) with similar functional groups to NIPMAM. This is followed by the simple and efficient precipitation polymerisation of NIPMAM and AA-CD to form a CD and NIPMAM based NG free of surfactant and comprising predominantly of NIPMAM. This process is illustrated as an overview in Figure 4.

To test the Nanogel, AZ was used as the model drug as the antimicrobial from Zernike produced is based of AZ. The loading and testing utilised UV/VIS spectroscopy and irradiation with 365nm light to determine the loading capacity of the nanogel and the typical induced release profile. To test the functionalisation efficiency of AA-CD HPLC-MS was used while Nile Red dye tests were used to prove the inclusion of CD in the NG product. For characterisation purposes FTIR, NMR, DLS and Zeta measurements were

conducted on the compounds and the CD-co-NIPMAM NG as well as the baseline NIPMAM nanogel without CD inclusion.

2.2.2 Preparation of β-Cyclodextrin for Co-polymerisation

Acrylate functionalisation of Ha-β-CD to prepare CD for use as an Nanogel co-monomer

2.2.2.1 Functionalisation of Ha-β-CD using EDC/NHS and AA

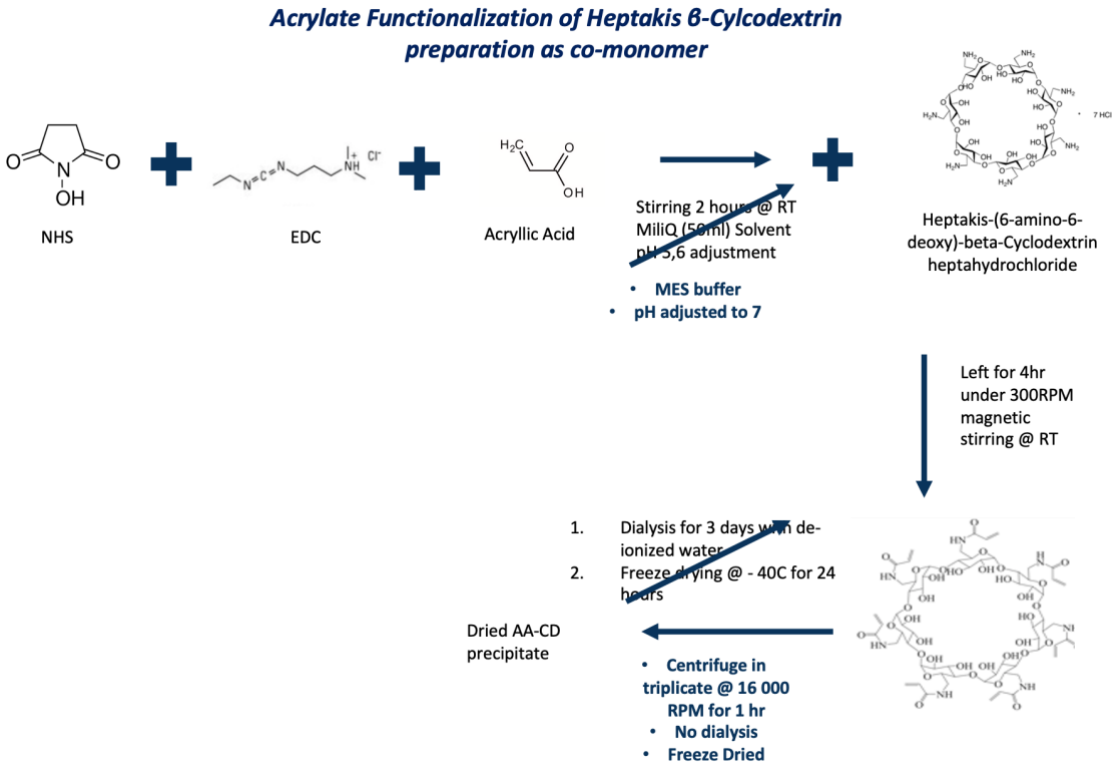

Figure 5 Schematic illustration of acrylate functionalisation of Ha-β-CD with EDC/NHS and acrylic Acid for use as a co-monomer in precipitation polymerisation. Images were sources from Sigma Aldrich or created in ChemDraw. Blue arrows in the diagram represent the adjustments to protocol in subsequent repeats made to improve the protocol.

A solvent of MiliQ was used for the acrylate functionalisation of Ha-β-CD. Repeat experiments used a non-amine and non-carboxylate buffer, MES, was used as a more appropriate buffer ([28]). This is indicated by the the blue arrows and texts in Figure 5 which shows the overall schematic. MES buffer is produced at a molarity of (0,1M) using MES and MiliQ. 390,3 mg of MES was added to 20ml MiliQ and the pH adjusted to 6 using a created solution of NaOH of 5M drop wise with iterative testing using a total of 140 µL. The NHS, EDC are warmed slightly by hand prior to weighing for ease of measurement and kept sealed in parafilm to mitigate the absorption of H_2O and corresponding weight increase. 38,4mg of EDC is added to 23,1 mg of NHS and 11mg of

AA in a small beaker with 10 ml of the MES buffer. This is left to stir 2 h and mix homogenously. This reaction was performed in darkness due to the photosensitivity of the EDC/NHS and the effect on efficacy of complete functionalisation of all 7 groups. This conjugation allows the couple of AA to NHS to form the AA-NHS intermediate ester for reaction with Ha-β-CD. The first of the two mechanism steps in this process of the EDC/NHS crosslinking reaction are the activation of the carboxyl groups on NHS forming an intermediate ester. This is followed the reaction of this intermediate with the primary amine bonds. After the coupling of AA to NHS achieved in the first 2 hours the pH is adjusted to 7 and 19,6 mg of Ha-β-CD is added slowly while stirring to allow for easy dissolving. This is left in the dark over night for 24 hours, at room temperature (RT), under constant stirring to produce the acrylate functionalised CD (AA-CD) where the NH_2 groups of Ha-β-CD are substituted with Acrylate groups from AA. This overall substitution creates a derivation of Ha-β-CD, AA-CD, with similar functional groups to NIPMAM thus allowing it to serve as a co-monomer in the polymerisation reaction during synthesis of the NG.

The AA-CD was stored in the freezer overnight and freeze dried at -40℃ for 24 hours thereafter. Dialysis was not conducted before synthesis of the AA-CD nanogel for simplification in the first attempt. Only one process of purification was completed after co-polymerisation on the Nanogel comprised of CD and NIPMAM (CD-co-NIPMAM NG) using centrifugation at 16000 RPM for 1 hr in triplicate. Subsequently, prior to use for characterisation by NMR and FTIR and the final co-polymerisation reaction, AA-CD was purified in an ice bath using acetone and further dialysed.

The above-mentioned amounts are to ensure NHS and EDC are in 3:4 molar ratio to the EDC/NHS mixture. A molar ratio of 2:1,5 of EDC/NHS to AA so that the reagents for CD are in excess. The CD:AA ratio needed was 1:7 in molar equivalence, however, to attempt full functionalisation of all 7 NH_2 groups of the β-CD an excess of AA is used in 1:10 of CD:AA. Only one process of purification was completed after polymerisation of Ha-β-CD and NIPMAM.

2.2.2.2 Functionalisation of Heptakis β-cyclodextrin directly with AA-NHS

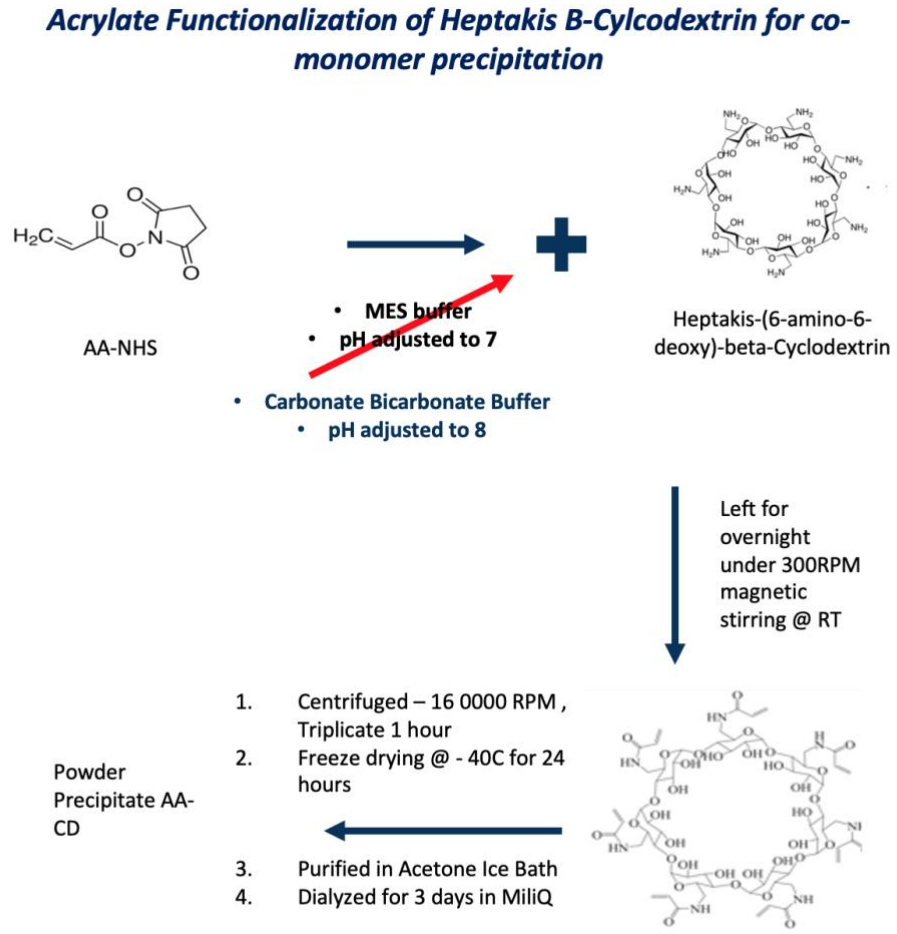

Figure 6 Schematic illustration of acrylate functionalisation of Ha-β-CD pre-modified AA-NHS for use as a co-monomer in precipitation polymerisation. Images were sources from Sigma Aldrich or created in ChemDraw. The red arrow in the diagram represent the adjustments to protocol in subsequent repeats made to improve the protocol.

For the functionalisation using AA-NHS the MES buffer was replaced by a carbonate-bicarbonate buffer. The overview of this process is depicted in Figure 6.Two solutions were made: 0,1M Na_2CO_3 was created using 1,06g of Na_2CO_3 in 100ml MiliQ (solution A) and 0,1M $NaHCO_3$ was created using 0,8g of $NaHCO_3$ in 100ml of MiliQ (solution B). A 20ml bicarbonate-carbonate buffer was made by adding 4ml of solution A to 16ml of solution B and adjusting the pH drop wise to 8 using 5M NaOH. The AA-NHS was kept sealed with parafilm and refrigerated. Preparation and storage techniques previously mentioned for AA-NHS were adhered to for this reaction. 95,84 mg of AA-NHS was added to the bicarbonate buffer solution and left stirring for 2 hours to fully dissolve and mix homogenously. 78,4 mg of Ha-β-CD is added very slowly while stirring to allow for easy dissolving. This reaction is left under constant stirring for 6 hours at RT to produce

the AA-CD. This reaction was performed with a 10:1 molar ratio of AA to Ha-β-CD to ensure excess presence of AA to attempt full substitution of all 7 NH_2 groups on Ha-β-CD with Acrylate groups. This reaction served the same purpose as the EDC/NHS reaction to prepare CD as a co-monomer for polymerisation. This reaction was carried out with AA-NHS that was purchased from Sigma Aldrich, already coupled with AA-NHS. This was done to mitigate any inefficiencies potentially experienced in the similar multi-step process utilising EDC and NHS with AA to form AA-NHS for the functionalisation reaction. These inefficiencies could come from several variables, most notably the photosensitivity of EDC in the reaction which was reported to affect the efficiency of the coupling and therefore the final substitution. This removed the need for a reaction in darkness for functionalisation and the need to wait for AA to couple to NHS to form an intermediate ester.

Initially, the AA-CD was stored in the freezer overnight and freeze dried at -40℃ for 24 h thereafter. Dialysis and purification were not conducted before the later synthesised AA-CD co-precipitated nanogel for simplification. Only one process of purification was completed after synthesis of CD-co-NIPMAM NG. This was achieved through centrifugation at 16 000 RPM for 1 hour, performed in triplicate prior to the freeze-drying step.

In further AA-CD synthesis replications, the AA-CD was first purified using precipitation in acetone over an ice bath. This was achieved by adding 250ml of Acetone to the solution over an ice bath at 4℃. Once the precipitate was formed this was filtered off into a conical flask, resuspended in 10ml MiliQ and dialysed using 1000kDa MWCO tubing. This was done for the purposes of testing and characterisation relating to FTIR/NMR and HPLC-MS of the AA-CD. This was followed by freeze drying at -40℃ for 24 h to produce a purified precipitate of AA-CD for characterisations steps and distribution analysis using HPLC-MS.

An additional NIPAM NG coupled with AA was crosslinked with Ha-β-CD based on a NG provided by Irem Soyhan within our research group. This was an alternative used to attempt to include CD in a NIPAM/NIPMAM NG. The method of first synthesising this AA-NIPAM NG as well as the crosslinking procedure to create the AA-NIPAM-co-CD NG is described in the List of Appendices, page 73.

2.2.2.3 Efficacy of Acrylate Functionalisation

To determine efficacy of the functionalisation, a distribution test was carried out on the purified AA-CD using HPLC-MS using a gradient column type in diluted acetonitrile as highly functionalised AA-CD is more hydrophobic and MiliQ is not a suitable solvent. This test was carried out to determine the distribution of the various possible outcomes of the acrylate functionalisation reaction. A schematic of the possible outcomes investigated using HPLC-MS is shown in Figure 7 below.

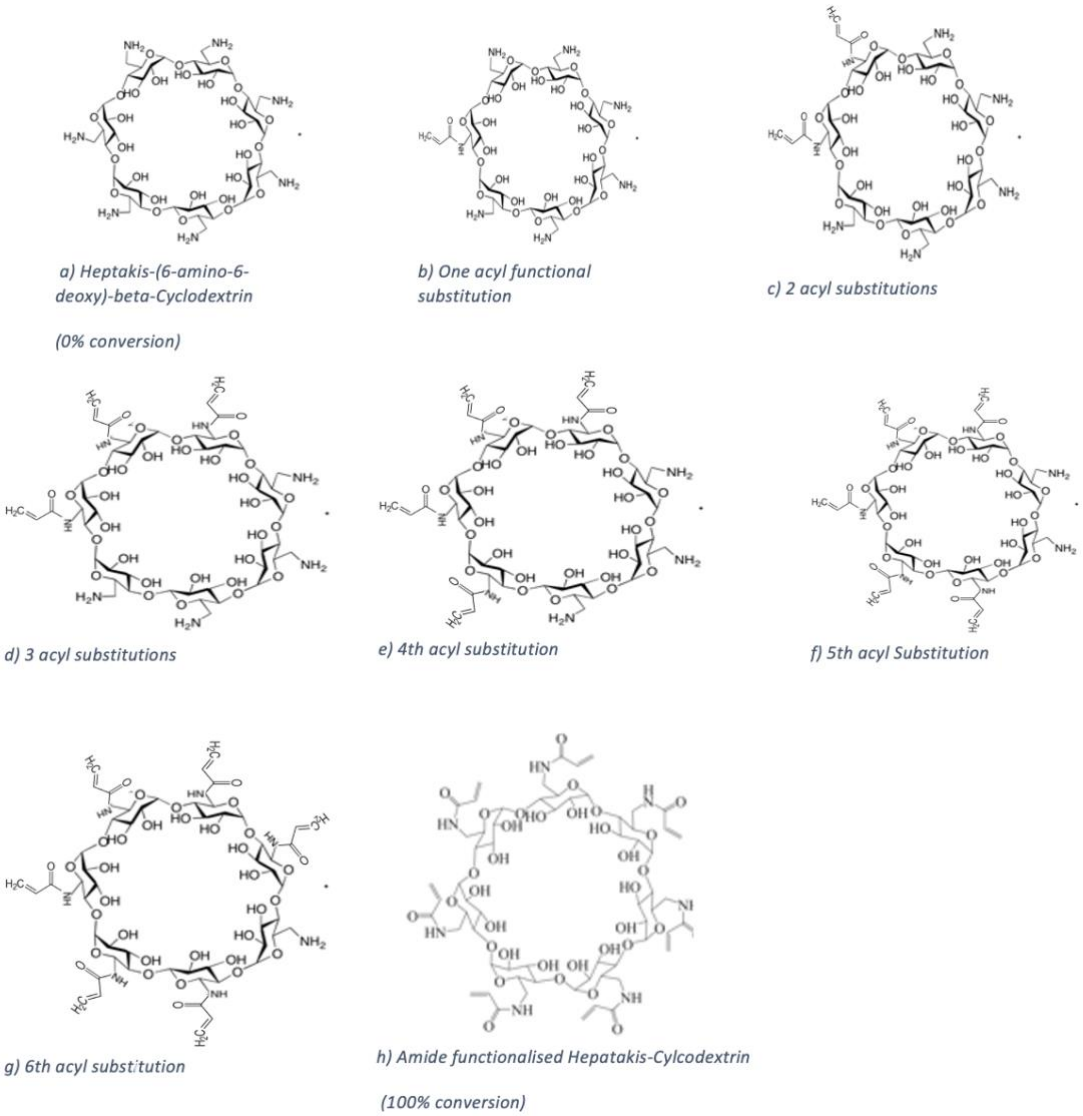

Figure 7 Potential target compound distribution from acrylate functionalisation of Ha-β-CD to AA-CD investigated to determine distribution and efficacy of reaction. Images were sources from Sigma Aldrich, modified or created in ChemDraw.

The efficacy of this reaction is being investigated to determine to what degree the functionalisation has been achieved and therefore percentage of highly functionalised AA-CD is produced for replication and potential isolation. The degree of

functionalisation will affect the cross-linking structure and density of the NG formed in precipitation polymerisation. This will affect and can be used to fine-tune the size, chemical composition, shape, rigidity, shrinking and swelling behaviour and stability of the NG formed. Additionally, this can affect the NG's response to its environment, drug entrapment and therefore controlled triggered drug release in drug delivery application. Moreover, this has key implications in the encapsulation of hydrophobic drugs, kinetic release of encapsulated drugs and cell uptake efficiencies ([23]). These are key considerations for the optimisation, testing and refinement of further adaptations of the CD-co-NIPMAM NG as a drug delivery platform for various other hydrophobic drugs and specific use cases of Zernike's AZ based antimicrobial drug.

2.2.3 Syntheses by Precipitation Polymerization

All NG protocols for synthesis follow the basic precipitation polymerisation technique shown in Figure 8 below for both pure NIPMAM NG's and the CD-co-NIPMAM NG's described in subsequent sections.

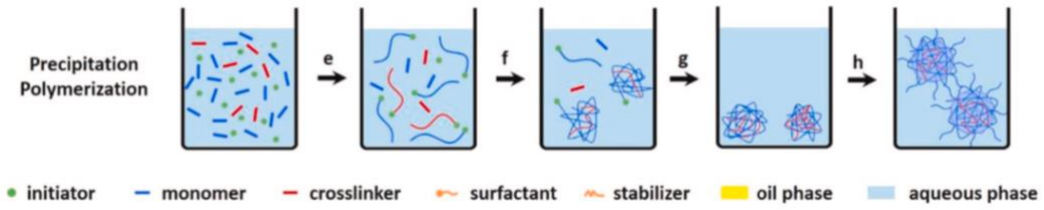

Figure 8 Precipitation polymerisation schematic description [12].

2.2.3.1 Precipitation polymerization of pure NIPMAM Nanogel

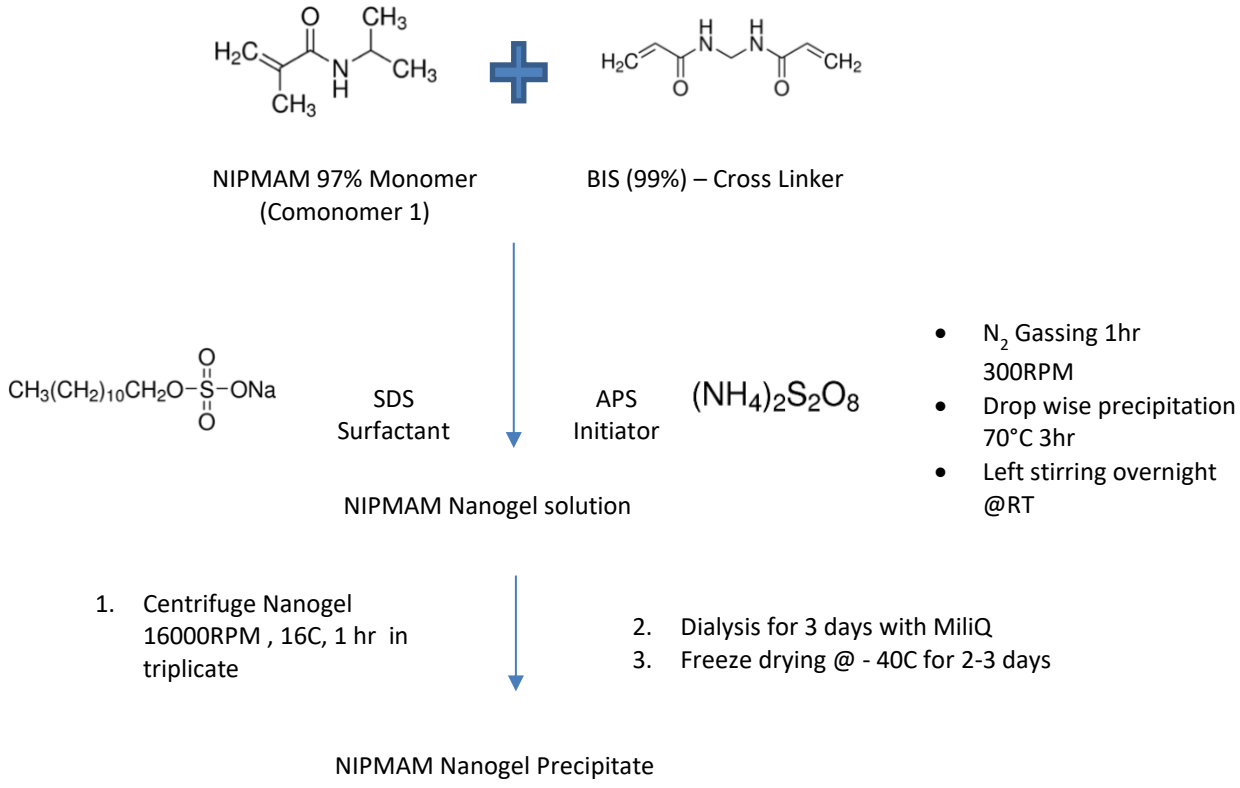

Figure 9 Schematic illustration of Polymerisation precipitation reaction for synthesis of NIPMAM nanogel. Images were sources from Sigma Aldrich, modified or created in ChemDraw.

The process was started with, 603 mg (4,8 mmol) of monomer NIPMAM, 39 mg (0,25 mmol) of cross- linker BIS, 23 mg (1,6 mmol) of surfactant SDS dissolved in 45mL MiliQ water. This was combined in a double neck round-bottom flask (250 mL) with magnetic stirring at 300 rpm. A reflux condenser with a nitrogen outlet was attached to one neck, the other neck was capped off by a rubber septum and used as a nitrogen inlet and outlet. The reaction mixture was degassed with N_2 for 1 h before heated to 70°C in an oil bath. Simultaneously a mixture of 11 mg (0,05 mmol) APS with 5 mL MiliQ was degassed in a separate flask at 300 rpm stirring for 1 h. The APS solution was injected smoothly into the reflux system after it was heated to 70°C. The reaction mixture underwent a phase transition from colourless to a turbid solution, indicating nanogel formation. This process was allowed to run for 4 h. The heating was then stopped, and the mixture was left under constant stirring for 24h. The method of choice is precipitation polymerization as shown in Figure 8 and **Error! Reference source not found.** above. Initially, this process was completed with 28mg and 36mg of SDS. The increased amount of surfactant in the first tests affected the cross-linker density of the nanoparticle causing the synthesis of a nanoparticle of smaller average diameter.

The 50 ml of the nanogel solution with BIS and NIPMAM was then dialysed using a dialysis tube with MWCO: 6-8 kDa cutoff, MiliQ water. Sealing issues occurred and triple folding of the tube ends was done to ensure the system was sealed. The Nanogel was dialysed for 3 days. The solution was then freeze-dried at -40°C for 24 h and the precipitate was collected. MiliQ water was replaced twice a day. In subsequent synthesis repetitions the nanogel was centrifuged at 16000 RPM (38 400rcf) for 1 h in triplicate and not dialysed.

Dynamic Light Scattering (DLS) was performed on the NIPMAM nanogel to verify literature expectations for synthesis size distribution and zeta potential. This process was repeated with 28mg and 36mg of surfactant and compared to literature values for NIPMAM nanogels ([11]). This is detailed further in section 2.2.4.1.

2.2.3.2 Co-Precipitation polymerization of CD-co-NIPMAM Nanogel

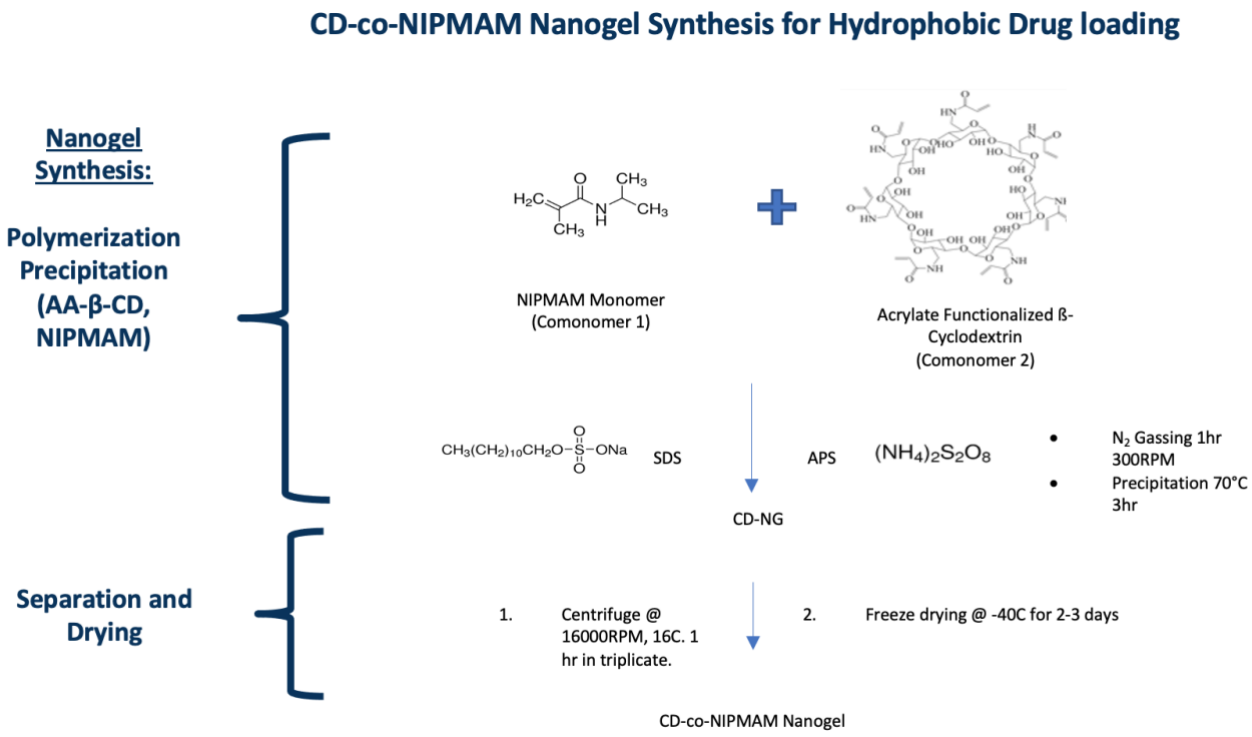

Figure 10 Schematic illustration of CD-*co*-NIPMAM nanogel synthesis, separation, and drying overview. Images were sources from Sigma Aldrich, modified or created in ChemDraw.

The co-precipitation overview is illustrated in Figure 10. This process was started with, 604 mg (4,8 mmol) of monomer 1 NIPMAM, 50 mg (0,0375 mmol) monomer 2 AA-CD, 39mg (0,25 mmol) of cross- linker BIS, 28mg (1,6 mmol) of surfactant SDS dissolved in 45 mL MiliQ water. This was combined in a double neck round bottom flask (250 mL) equipped with a stirrer bar at 300 rpm.

The processes described previously were repeated with N_2 gassing for 1 h of the APS and polymer solutions separately. The 3-neck flask with both copolymers, surfactant (SDS) and BIS cross linker, was connected to a reflux condenser, suspended in an oil bath, and heated to 70 ° C with magnetic stirring at 300 rpm. Once heated to 70°C, the APS solution was injected smoothly into the 3-neck flask and the reaction allowed to proceed for 4 h. Thereafter, the solution was allowed to return to RT with continual stirring overnight.

The cloudy phase transition was observed and the AA-CD-*co*-NIPMAM NG was removed and centrifuged at 16℃, 16000 rpm (38 400rcf) for 1 hr in triplicate to remove insoluble

reagents. The nanogel stock was resuspended and was dialysed using MWCO: 6-8 kDa cut-off tubing with MiliQ for 3 d. This precipitate was then freeze dried overnight (24 h) at -40°C and the nanogel powder was recovered and stored under refrigeration at 4°C.

2.2.4 Characterisation, Verification and Drug Modelling

2.2.4.1 Dynamic Light Scattering (DLS)

DLS measurements were conducted on the NIPMAM NG's synthesised with various SDS amounts and the CD-*co*-NIPMAM NG using the (Malvern ZetaSizer ZS, Model: ZEN3600). All measurements were done in triplicate. The average size was determined for all NIPMAM nanogels and for the CD-*co*-NIPMAM NG. Zeta potential measurements were taken of all four NG's to determine the average. Additionally, a temperature sequence measuring average size was utilised for both the final NIPMAM and CD-*co*-NIPMAM NG's utilising the amount of SDS in synthesis. This was measured from 20°C to 60°C in 2°C intervals following the particle count and average measured size. From these graphs the VPTT and change in VPTT were calculated.

2.2.4.2 Ultraviolet/Visible Light (UV/VIS) Characterisation – Drug loading test

Firstly, UV/VIS analysis was conducted on the various compounds used to construct standard curves to be used later for molarity calculations and comparisons. Prior to use all AZ solutions were heated in hot water baths for 24 hours, with water replacement. This ensured full conversion of the AZ to its stable TRANS conformation suitable for hydrophobic inclusion and the measurement of one defined peak at 350nm. To ensure acceptable S/N ratios in measurements, preparation tests were conducted to find acceptable concentration limits. All measurements were conducted using Quarts cuvettes across a 250 to 700nm spectrum using the DLS (Malvern ZetaSizer ZS, Model: ZEN3600). Further testing used concentrations correlating to an absorbance of less than 1 to ensure reliability of the data and acceptable noise to signal ratios. Each DLS run used a double blank of MiliQ to ensure that calibration was consistent. A verification was conducted on β-CD to check no absorbance was measured. Calibration curves were constructed by using 0,0046mmol/ml of AZ, 8,85mg/ml of NIPMAM NG and CD-*co*-

NIPMAM NG. Five equal dilutions of each of these solutions were measured to construction a concentration calibration curve for each compound. This was done to create controls to understand the relative relationship between absorbance and concentration for each compound. These curves were used to correlate later absorbance measurements in drug loading tests with known concentration values.

B-CD was incubated overnight with 1:1 molar ratio of AZ (4,6μmol/ml) and centrifuged before DLS was conducted on the sample to determine if any shift occurred with the inclusion. A test for atypical binding was conducted on the NIPMAM nanogel by incubating a solution of 0,0046mmol/ml AZ with the NIPMAM NG overnight. This was then centrifuged in triplicate with Beckman Coulter JSS13E27 centrifuge for 1 hr at 16000 RPM (38 400rcf) and 16°C. The resulting supernatant absorbance of AZ was measured and compared with the origin concentration of AZ loaded with the NIPMAM NG.

A sequence of centrifugation and washing was run on a solution of CD-*co*-NIPMAM NG and AZ to determine the loading capacity/efficiency of the nanogel. Assuming full inclusion of CD, the molar ratio of 128:1 from co-precipitation was assumed. Equal molar amounts of AZ and CD within the NG complex were used for incubation and testing. 0,0025mmol/ml AZ was incubated overnight with 8,85mg/ml CD-*co*-NIPMAM NG. Each sequence step consisted of centrifugation at 7800 RPM (7400rcf) and 4°C followed by supernatant removal and resuspension in MiliQ. Each supernatant was measured to determine the AZ concentration until the supernatant absorbance was zero. The remaining CD-*co*-NIPMAM NG absorbance was then measured. This was done to remove loosely bound AZ from NG complex until only encapsulated and bound AZ inside the CD hydrophobic pocket remained and the loading capacity could be determined compared to the original AZ concentration in incubation.

Simultaneously, AZ and CD-*co*-NIPMAM NG of the same molar concentrations and the solution was then dialysed in dark in MWCO: 6-8 kDa cut-off tubing with MiliQ for 4 days. The MiliQ was replenished twice a day. The remaining NG solution absorbance was measured to determine loading capacity in a less harsh method. Additionally, this was a test to determine if AZ was being ripped out of the CD pocket from the high centrifugal force used in centrifugation.

2.2.4.3 Ultraviolet/Visible Light (UV/VIS) Characterisation – Triggered release test

The dialysed and centrifuged CD-*co*-NIPMAM NG complexes loaded with AZ were then irradiated with 365nm to change the AZ from its TRANS to CIS conformation. This converts AZ to a weakly bound conformation that triggers its release from the hydrophobic pocket of CD. This is also the same trigger for the activation of the AZ based antimicrobial drug the hydrophobic vector is being designed for. Samples were kept in the dark in ice baths at 4 ° C for the duration of the experiment.

Each sample was irradiated with a handheld lamp with 365nm wavelength for 1 minute. Following this, the supernatant was measured to determine the concentration of AZ and therefore the amount of AZ. The solution was centrifuged at 16 000 RPM (38 400rcf) and 4°C for 30 minutes. The supernatant was remeasured, and the NG complex was resuspended. This sequence was repeated until there was no longer an absorbance of AZ measured from the supernatant. A time profile of triggered release was developed from this data.

2.2.4.4 Fourier Transformed Infrared (FTIR) Spectroscopy

A KBr pellet based FTIR machine (Agilent Cary 670 and sliding Wear Tester TR-17, Ducom) was used for spectral analysis of the synthesised compounds and NG's as well as unmodified compounds used in the synthesis procedures. 100mg background KBr pellets were pressed using a mechanical press for removal of background spectra in the analysis. All compounds measured by FTIR were in dry powder form. Pellets of 100mg were produced of each compound 98:2 weight % of KBr to each dry powder compound. FTIR spectrum measurements were taken of the AA, AA-NHS, β-CD, Ha-β-CD, AA-CD, NIPMAM NG's of various sizes and the CD-*co*-NIPMAM NG. Spectral measurements were exported to excel for comparative graphing and analysis. Spectra were compared with literature to identify and verify the presence of functional groups of each compound and the presence of CD within the CD-*co*-NIPMAM NG.

2.2.4.5 Hydrogen Nuclear Magnetic Resonance Spectroscopy (H-NMR)

NMR was performed on AA and CD products to identify that the acrylate functional of AA had been fully activated in the process and that the Ha-β-CD was successfully functionalised. The spectra were analysed for determination of extent/efficiency of functionalisation of AA-CD by determining the number of NH2 terminals replaced by acrylate groups. AA, the NIPMAM NG and Ha-β-CD were used as controls for these observations and the results were compared with literature expectations. NMR was conducted on the CD-*co*-NIPMAM and characteristic peaks were compared with literature expectations for specific bond vibrational frequencies, this spectrum was then compared with the NIPMAM NG without CD.

The product was characterized with 1H NMR (JEOL, GSX, 500 Hz) with deuterated dimethyl sulfoxide and heavy water (deuterium oxide) at 25°C and with IR measurements (IR spectroscopy; Hitachi 260-10). Similarly due to increased hydrophobicity of the higher functionalised AA-CD, this was attempted in chloroform as water showed poor solubility.

3 Results

3.1 Average size, Zeta potential and VPTT of NIPMAM and CD Nanogels from DLS

3.1.1 Average Size and Zeta Potential

Adjustments to SDS molar ratios within precipitation polymerisation capped the growth of the particles in synthesis and influenced cross linker density of the NG, resulting in lower average sizes for the NG complex synthesised with high surfactant concentration. The NG comprised of greater average particle diameter showed a greater intermolecular interaction resulted in a 25% absolute reduction average zeta potential. The lower concentration of SDS caused a lower crosslinker density and a less tightly bound NG complex, resulting in a NG complex of higher average hydrophobic diameter. Measured Zeta potentials of the two NG complexes of different surfactant concentration had little difference. The hydrodynamic diameters of the NIPMAM NG's were 415,5±16,3nm and 266±6,5nm for the low and high surfactant protocols respectively. These were measured in triplicate with average PDI's of 0,09±0,04 and 0,04±0,03 and therefore considered reliable data measurements. Measured zeta potentials for these nanogels were -21±2mV and -18,8±0,9mV respectively. These results are represented in Figure 11 below.

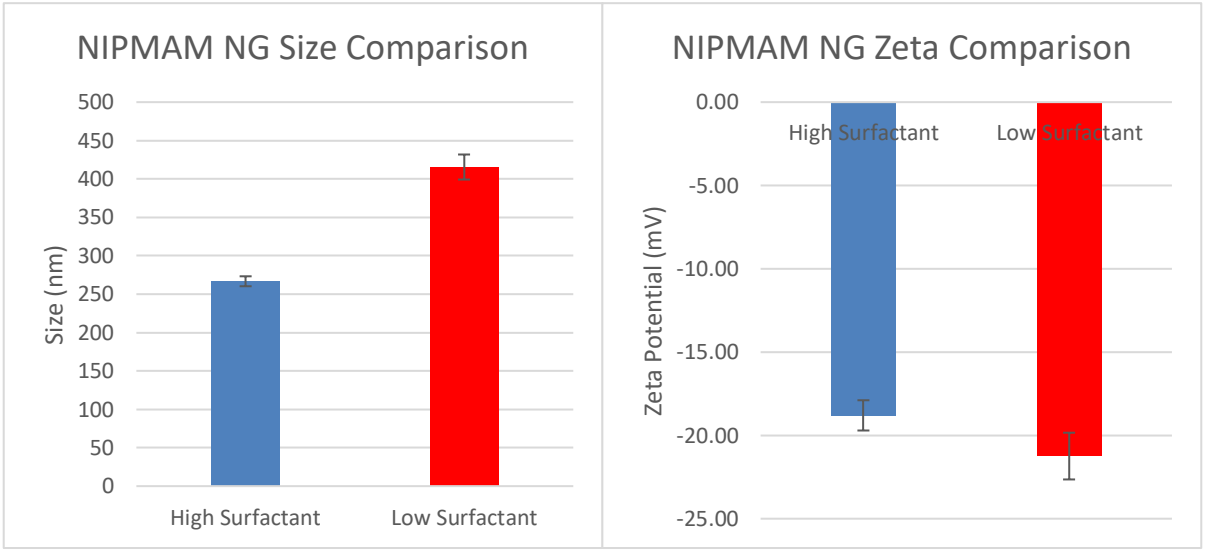

Figure 11 Average Size and Zeta Potential Measurement from DLS for NIPMAM NG using high SDS (28mg) and low SDS (23mg) synthesis approaches. Average hydrodynamic diameter measurements were taken at 24°C.

The hydrodynamic diameter of the NG complex increased from 415,5±16,3nm for the NIPMAM NG to 1052±6,9nm for the CD-*co*-NIPMAM NG with the addition of the CD in the polymer network at 24°C. The PDI of the measurements for CD-*co*-NIPMAM was 0,104±0,03. The measured zeta potential of CD-*co*-NIPMAM NG at 24 was -18,5±0,4mV and -15,5±0,2mV. No significant change in zeta potential was measured between the high surfactant synthesised NIPMAM NG and the CD-*co*-NIPMAM NG. These results are represented and compared in Figure 12 and Figure 13 below.

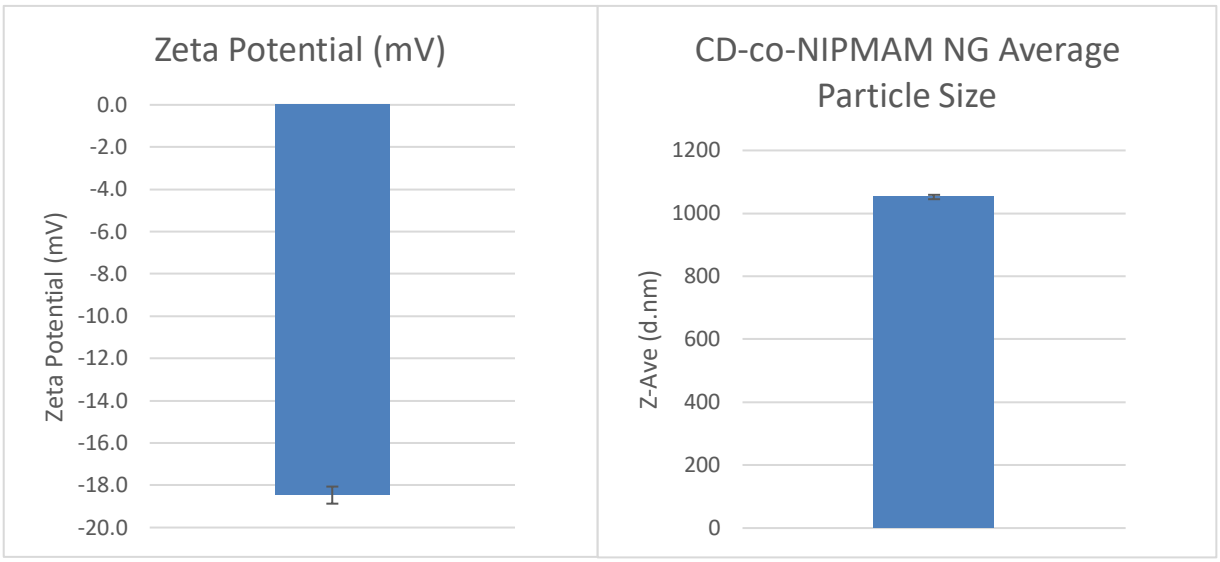

Figure 12 Average particle size distribution and Zeta potential measurements for CD-co-NIPMAM NG at 24°C. This figure represents the co-polymerised NG formed through a high surfactant protocol.

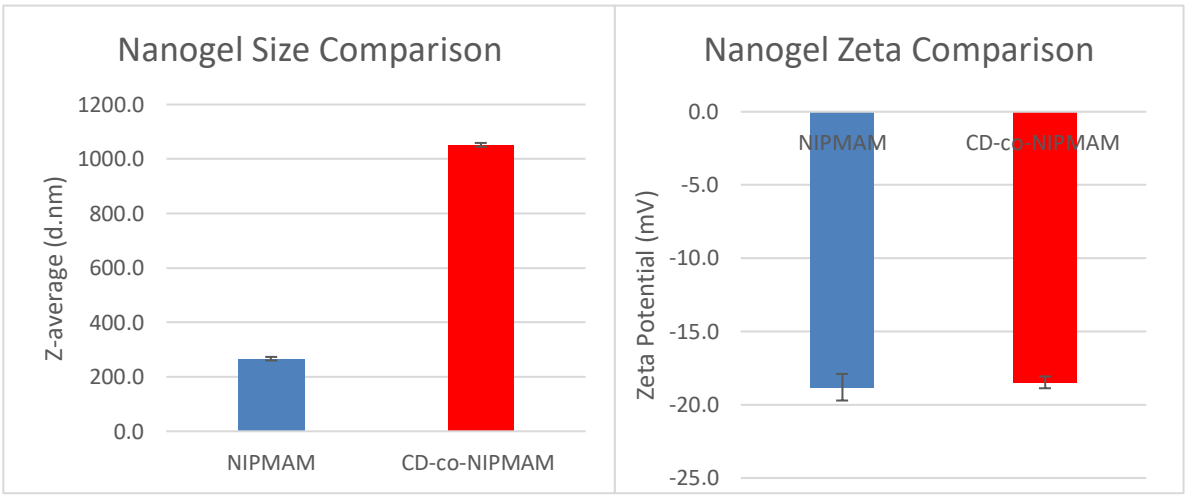

Figure 13 Comparison of average hydrodynamic diameter (d.nm) and Zeta potential (mV) of NIPMAM NG and CD-co-NIPMAM Nanogel for high sufractant concentrations in synthesis (23mg SDS). These were all conducted at 24°C

3.1.2 VPTT measurements for NIPMAM and CD-*co*-NIPMAM NG's

The resulting temperature dependant nanoparticle size distribution for NIPMAM NG synthesised with low surfactant (SDS) concentration showed a size/volume change over the temperature range of 38°C to 52 °C. The decreasing average particle size indicates a volume phase transition range, a VPTT of approximately 45°C for the complex. Similarly, the temperature dependant distribution for the high SDS concentration based NIPMAM NG indicated a VPTT of approximately 46°C. These are depicted in Figure 14 and Figure 15 below.

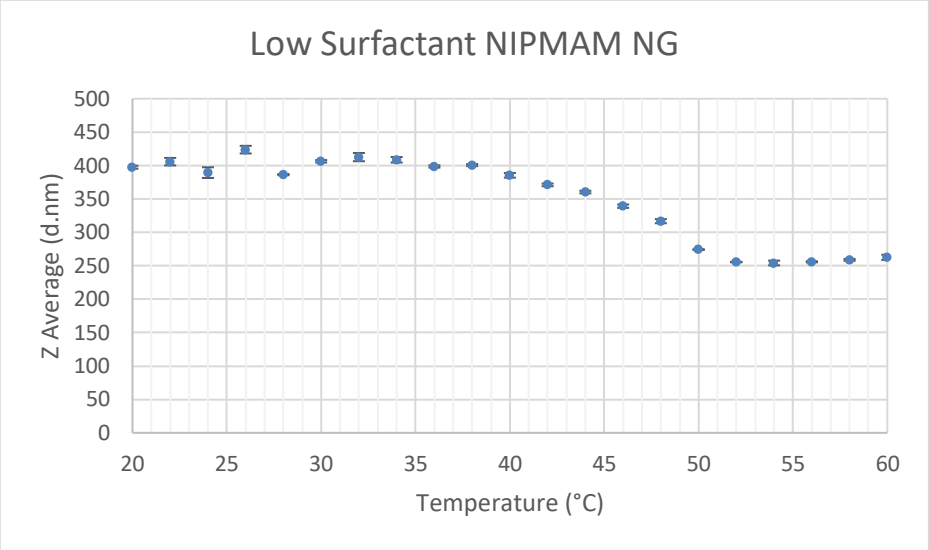

Figure 14 Temperature trend of average diameter for Low SDS NIPMAM NG approximating the VPTT of the complex. Average hydrophobic diameter measurements for NIPMAM NG over a temperature range of 20 to 60°C in 2°C increments.

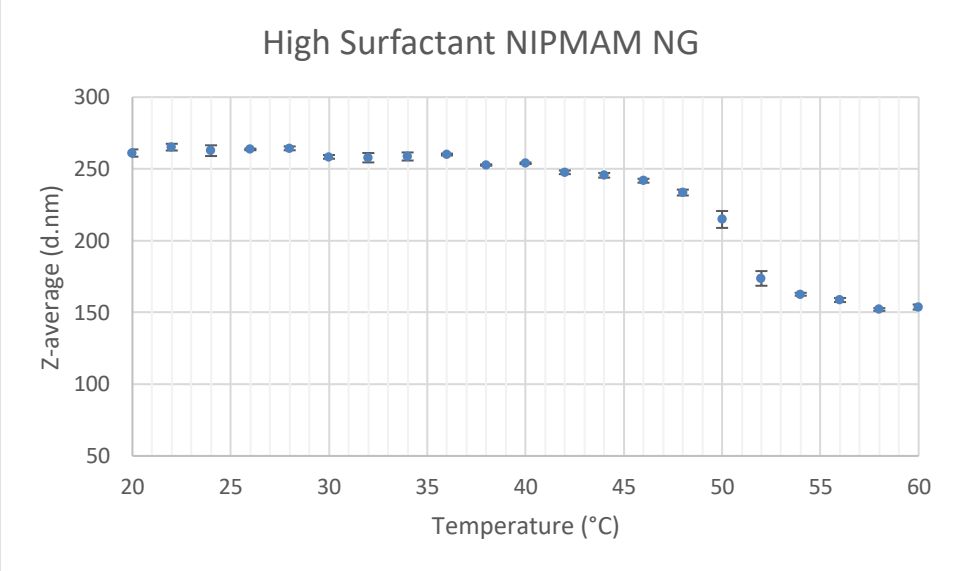

Figure 15 Temperature trend of average diameter for High SDS NIPMAM NG approximating the VPTT of the complex. Average hydrophobic diameter measurements for NIPMAM NG over a temperature range of 20 to 60°C in 2°C increments.

Comparatively, the resulting temperature dependant nanoparticle size distribution for CD-*co*-NIPMAM NG illustrated an identifiable size reduction over the range of 36°C to 58 °C indicating, through a linear trendline over the phase transition range, a VPTT of around 47°C. This is illustrated in Figure 16 below.

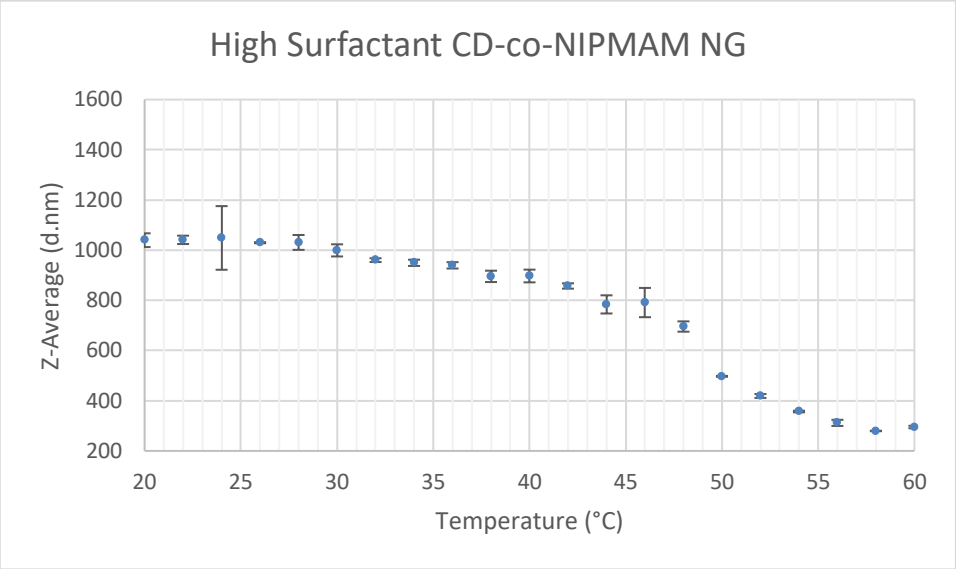

Figure 16 VPTT measurement of CD-*co*-NIPMAM NG. Average hydrophobic diameter measurements for CD-*co*-NIPMAM NG over a temperature range of 20 to 60°C in 2°C increments.

3.2 Primary characterisation from HNMR

No measured spectral peaks were apparent in the NMR for the AA-CD or the CD-*co*-NIPMAM NG to indicate functionalisation or inclusion of the CD in the NG complex respectively. These results are shown in , Figure 17, below. Various solvents were used from DMSO, water to chloroform. Inability to gain NMR results for functionalised CD (AA-CD) and the CD-*co*-NIPMAM NG were ubiquitous regardless of solvent used. These issues with NMR for analysis were experienced by other investigations in the group and the method was forgone in favour of the non-quantitative and less accurate FTIR analysis to attempt to verify functionalisation of AACD and validate the inclusion of CD in the CD-*co*-NIPMAM NG complex. No further NMR testing or analysis was conducted.

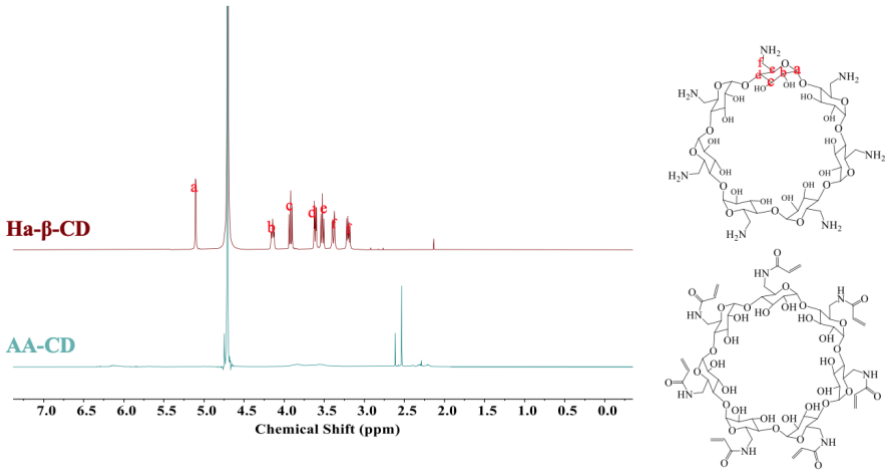

Figure 17 NMR spectrum comparison of Ha-β-CD vs Functionalised CD (AA-CD)

3.3 Secondary characterisation by FTIR

Figure 18 shows the overlay of the FTIR spectra of Ha-β-CD and AACD for qualitative comparison of functional group changes. The results showed changes in the characteristic pattern of absorbance bands between Ha-β-CD and AACD. Specifically, the vibrational and rotational energy bands represented by the wavenumbers illustrated by arrows and peaks corresponding to; N-H (3369 cm^{-1} and 3302$cm^{-1)}$, C=O (1679 cm^{-1}), C=C(1640 cm^{-1}), C-N(1240 cm^{-1}), N-H (1609cm^{-1}) and the glucopyranose ring (700-1000 cm^{-1}). These changes in the characteristic pattern of absorbance bands for AA-CD indicate the successful functionalisation of Ha-β-CD where the NH_2 functional groups have been substituted with acrylate groups. Specifically, the C=O (1679 cm^{-1}) would represent the highly characteristic band with associated with the amide stretching of AA-CD. However, this is a non-quantitative method of analysis. As a result, it is inconclusive regarding the degree of functionalisation of all 7 target groups on Ha-β-CD and the mass distribution of the possible outcomes of the EDC/NHS and AA-NHS reactions. HPLC-MS analysis was conducted for further information on the success and distribution of this reaction.

Figure 19 shows the overlay of the FTIR spectra for AACD, the NIPMAM NG and CD-*co*-NIPMAM NG as a qualitative comparison. The results show a near identical characteristic pattern of absorbance between the NIPMAM NG and the CD-*co*-NIPMAM NG complexes. Specifically, attention is drawn to the lack of appearance of the bandwidth pattern associated with the glucopyranose ring present in the in AACD spectrum indicated by the segment between the two vertical dashed lines. This characteristic pattern was expected in the CD-*co*-NIPMAM NG spectrum should CD have been successfully included in the NG complex through co-precipitation polymerisation. Variations were experienced in repeat FTIR spectra analyses for AACD. As result all spectra obtained for AACD were reviewed or considered to minimise possible errors.

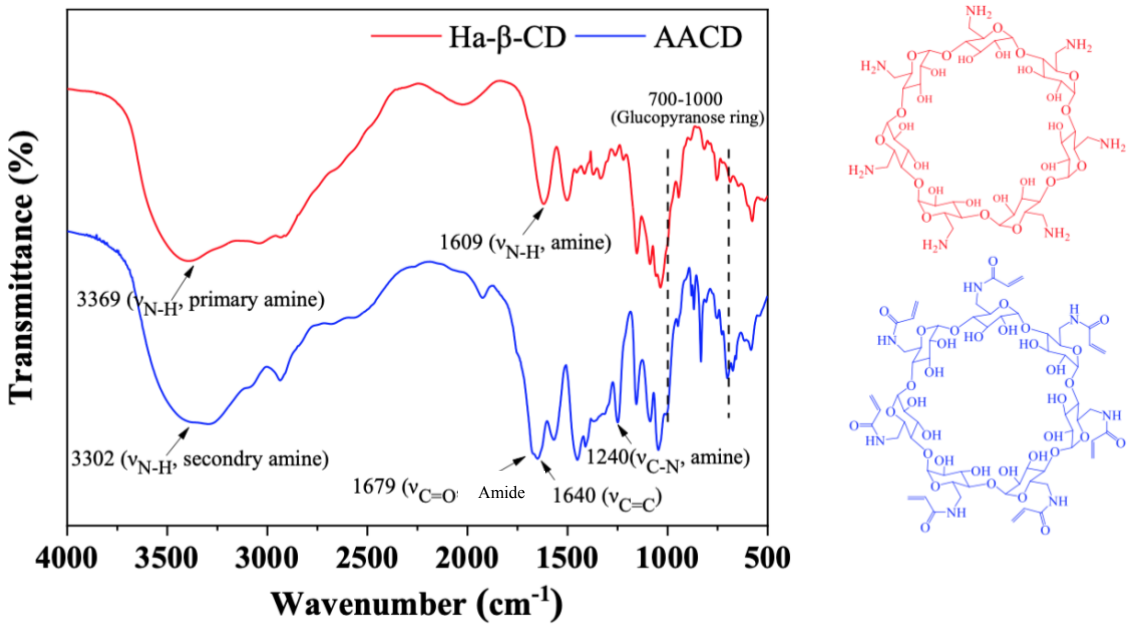

Figure 18 FTIR spectrum of Ha-β-CD vs functionalised Ha-β-CD (AA-CD) showing the functional group modifications from NH2 to Acrylate groups

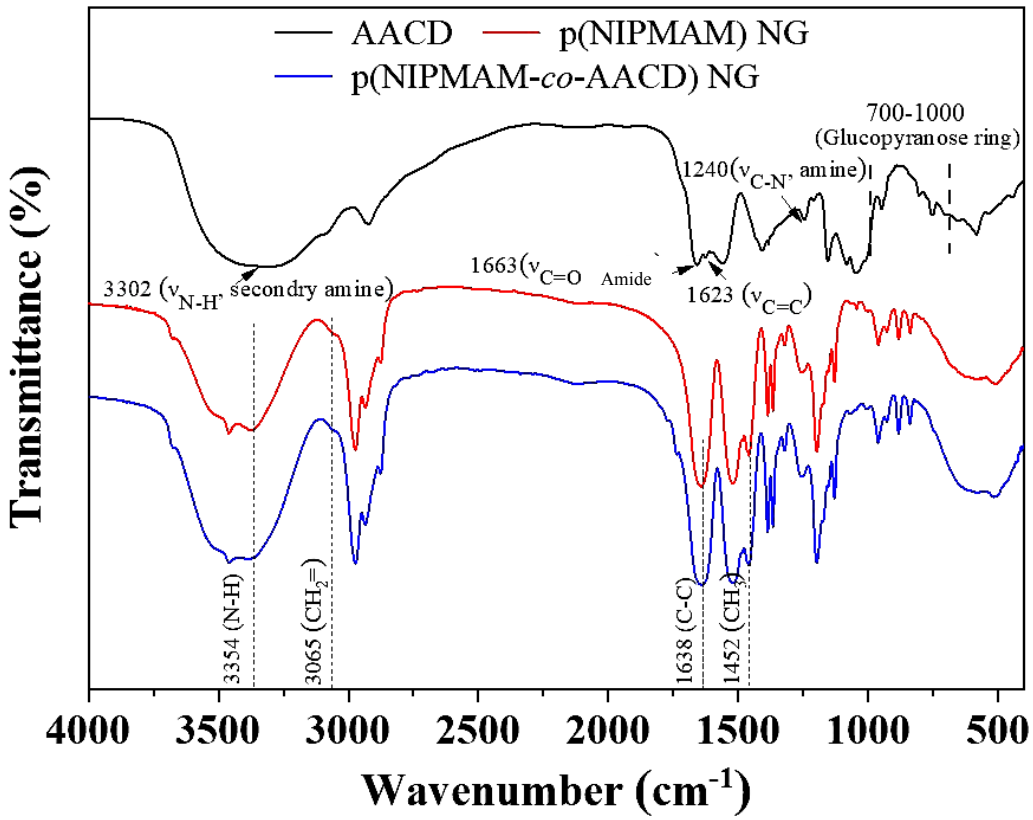

Figure 19 FTIR Spectra of NIPMAM NG, CD-co-NIPMAM NG (pNIPMAM-*co*-AACD) and Functionalised CD (AACD) with characteristic peaks and localisation of expected glucopyranose ring due to presence of CD

As can be seen from the additional EDC/NHS crosslinking reaction utilising NIPAM-co-AA and Ha-β-CD the observed FTIR spectra showed a change in the characteristic absorbance pattern resulting in the appearance of the glucopyranose ring structure between 700 cm^{-1} and 1000 cm^{-1} as found in the Ha-β-CD. This is shown in Figure 20, below. While not conclusive, this indicated the potential successful inclusion of CD in the NIPAM NG complex through the cross-linking reaction unlike the resulting FTIR spectral overlay observed from the co-precipitation polymerisation reaction with NIPMAM and AACD.

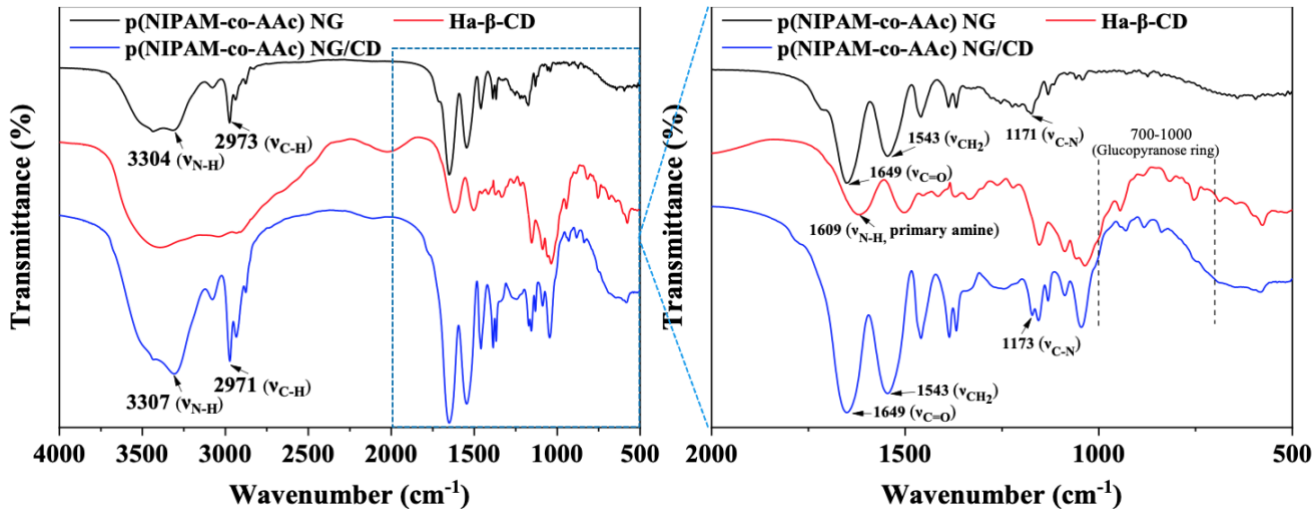

Figure 20 FTIR Analysis of AA-NIPAM NG coupled with Ha- β-CD showing spectra groups for the inclusion of cyclodextrin in the EDC/NHS coupled synthesis method

Table 1 FITR Absorption bands of different functional groups for NIPAM-*co*-AAc nanogel G-1, G-2, G-3

Functional groups	Observed peaks for G-1 (cm^{-1})	Observed peaks for G-2 (cm^{-1})	Observed peaks for G-3 (cm^{-1})
C–N	1148.00	1151.78	1154.56
CH_2 (b)	1549.67	1535.53	1535.53
C—O (amide)	1615.64	1621.83	1625.78
C–H (s) sp^3	2971.35	2966.32	2954.43
N–H (s)	3307.00	3311.50	3308.47

3.4 UV/VIS

3.4.1 Standard Curves and Loading Capacity

3.4.1.1 Constructed Standard Curve for AZ

Figure 21 was constructed using UV/VIS spectra found in Appendix 1, 65. Absorbance was maintained around a maximum of 1±15% to ensure that the signal / noise ratio (S/N) was within acceptable limits to provide reliable data. Figure 21 was used for conversion of spectra absorbance readings in the AZ loading and atypical tests to mM contributions of observed peaks. This graph was used to create AZ stock solutions used for loading of the CD-*co*-NIPMAM NG to ensure that the S/N ratios were within acceptable limits when 1:1 molar ratios of AZ to CD were used in the nanogel complex. The molarities of the supernatants in atypical binding and CD-*co*-NIPMAM loading were derived from the figure above.

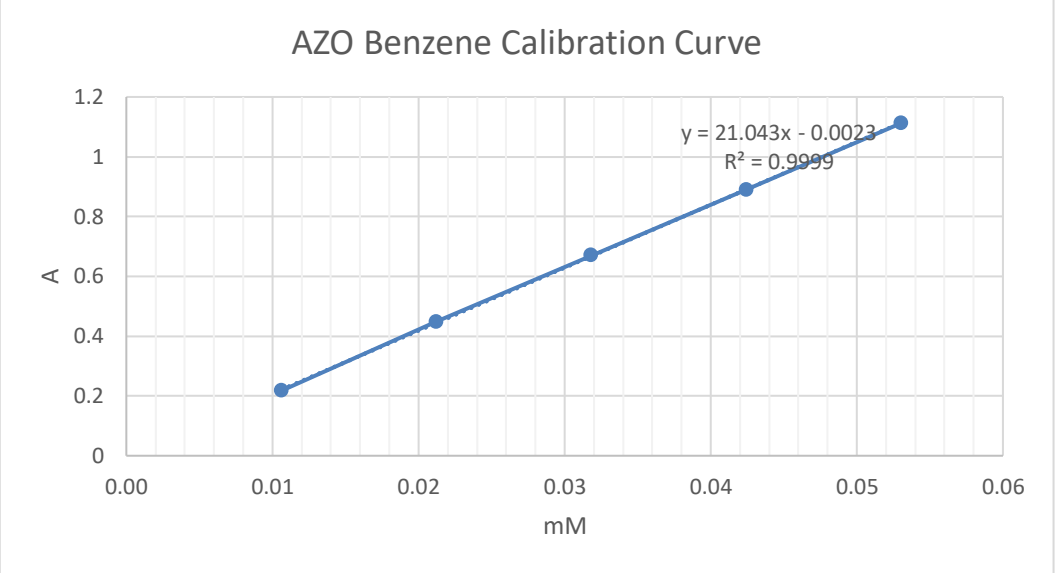

Figure 21 UV/VIS Standard Curve constructed for Azo Benzene at various molar concentrations, measured between 250nm and 700nm.

3.4.1.2 Atypical binding and CD-*co*-NIPMAM loading capacity

After 0,87mg (2,5μmol) of AZ was incubated with 8,75mg of NIPMAM NG for 1 day in 50ml. This test was carried out in triplicate. The solutions were centrifuged in triplicate for 1 hr at 16 000 RPM (38 400rcf). Table 2 shows the results of the atypical binding tests for the base NIPMAM NG. The summary of the atypical binding results comparing absorbance of the loaded AZ vs the supernatant measurements, indicating a decrease in absorbance intensity of AZ, can be found in List of Appendices, page 66-69. The corresponding molarity of AZ in the supernatant was derived from the standard curve in Figure 21. The results showed that without the inclusion of CD's hydrophobic pocket in the NG complex there was atypical binding or entrapment of AZ within the NG complex of approximately 6,59 ± 0,46%. No significant shift in wavelength of the peak was observed. These results and spectral overlays can be found in the List of Appendices, page 66-69.

Table 2 Results for triplicate of Atypical binding test for AZ with NIPMAM NG

	Atypical test 1	Atypical Test 2	Atypical Test 3	Average
Atypical Binding %	6,99	6,08	6,70	6,59 ± 0,46

0,85mg of (0,0024mmol) in 50ml of MiliQ of AZ was incubated with 8,85mg of CD-*co*-NIPMAM NG overnight. After 5 days of dialysis in MIliQ the NG solution measured a reduction in absorbance of 6,58 % on a molar basis which indicated a loading or binding of 6,58% of AZ within the NG complex. No shift in absorbance peak was observed in the UV/VIS spectra nor a significant peak at the expected wavelength, 350nm, characteristic of AZ in its TRANS conformation.

Table 3 Loading test for AZ with CD-co-NIPMAM NG at approximate 1:1 molar ratio

	Wavelength of Peak (nm)	Absorbance	mM	Loading/Bound as % of initial AZ added
Total Absorbance of loaded NG after Dialysis	350	1,11	0,053	6,58
Absorbance contribution of NG	350	1,03	0,049	
Difference → Loaded/Bound AZ	350	0,07	0,003	

3.4.2 AZ Triggered release with Irradiation

No experiment was followed with triggered release of AZ from the CD-*co*-NIPMAM nanogel. Inconsistent data was collected from the centrifuge-based protocol for loading capacity testing of the NG complex with CD. The dialysis alternative showed, after 5 days, that the remaining AZ retained in the NG complex was approximately 6-7% of the original molar amount of AZ added. This was approximately the same as the expected atypical binding of the NIPMAM Nanogel without CD. A light induced conformational change was determined to be unnecessary as it would not trigger AZ's release and no release profile protocol was followed thereafter. Alternative testing and synthesis considerations needed before attempting triggered release are described in the Clinical Relevance, Limitations and Recommendations section. Further points and reflection on expected outcomes of triggered testing can be found in the List of Appendices, page 71-72.

4 Discussion

4.1 DLS/Zeta and VPTT Measurements

Two protocols for precipitation polymerisation were followed according to known literature expectations for known molar ratio of surfactant, crosslinker, initiator and the polymers. This was done to ensure, prior to co-polymerisation using a limited β-CD resource, that methodology was repeatable, and the sufficient understanding and success was achieved. Furthermore, basic NIPMAM NG's were synthesised to create a reference point for average hydrodynamic diameter, zeta potential and VPTT measurements in order to identify and characterise any shifts or effects created by the potential inclusion CD in the target NG complex. Following the success of these NG formations, CD was functionalized in preparation as a co-monomer for copolymerisation in the final target NG for hydrophobic drug loading and testing.

While the sizes vary significantly, β-CD and its derivatives have large cavity (hydrophobic pocket) diameters of approximately 0,6 to 0,65nm and heights of 0,75nm ([26]). If CD was included successfully, it could be expected that the average hydrodynamic diameter of the NG complex would illustrate a change due to possible variation in structural formation during synthesis. The lower concentration of SDS caused a lower crosslinker density and a less rigid NG complex, resulting in a NG complex of higher average hydrodynamic diameter. Measured Zeta potentials of the two NG complexes of different surfactant concentrations showed marginal statistical differences. The results for both NG's for average hydrodynamic diameter and zeta potentials for known synthesis protocols agreed with expected literature values ([11]). The DLS results showed a 154% increase in average measured particle size for the CD-*co*-NIPMAM NG at low SDS concentration compared to the NIPMAM NG of the equivalent SDS molar concentration in synthesis. The increase in average hydrodynamic diameter was an initial indicator that CD had been included in the NG complex. However, this can be due to several confounding variables such as aggregation and impurities during measurement, although aggregations would likely have resulted in large PDI's and multiple intensity peaks which was not observed. All PDI's found to be in acceptable limits between 0,04

and 0,104 and the data deemed reliable. Inclusion was therefore further analysed in VPTT, primary and secondary characterisation techniques.

Temperature-dependent size distribution tests using DLS showed slight changes in the VPTT between the low-surfactant NIPMAM NG, high-surfactant NIPMAM NG, and the CD-*co*-NIPMAM NG. The VPTT of NIPMAM only nanogels, as known according to the literature, are expected to be in the range of 43 ° C to 45 ° C. The VPTT's approximated from DLS measurements on the NIPMAM and CD based NG complexes were 45°C, 46°C and 47°C. When modifications of NIMPAM NG's are achieved we expect the VPTT to shift due to increased energy needed to break the molecular interactions and bonding formed between CD and NIPMAM. This process favours the interaction of polar groups of the NG with the polar solvent, water and the apolar intermolecular interactions of the copolymer's groups. This causes the collapse of the nanogel or shrinking as solubility changes. The addition of CD influences the additional intermolecular forces to be overcome in this process for collapse to occur. Changes in the VPTT can therefore usually be attributed to modifications made to a NIPMAM NG, the contribution of which depends on the molar equivalence of the modification. Although slight variations were observed, it is hypothesised that these are merely due to the variance in accuracy of the measurement procedure as well as inaccuracy of the linear trend fits used for approximating the VPTT of the complexes. Furthermore, the slight increase in VPTT observed in the CD-*co*-NIPMAM NG compared to the NIPMAM NG's could not be conclusively attributed to or therefore serve as partial validation of the inclusion of CD in the NG complex. Additionally, while its simple to define a single point at which phase transition occurs this is not necessarily the case for a real system. In a real system the phase transition occurs over a range of temperatures. This is because of the polydispersity which stems from several variables such as differences in chain lengths, branching, cross-linking etc ([3,22]). The shrinking behaviour or characteristics of the NIPMAM and CD-co-NIPMAM may further differ based on the hydrodynamic diameter, polydispersity and structural variance. Differences in the slope and degree of swelling and shrinking can be seen in the VPTT diagrams. The CD based NG of larger average diameter shrinks to a larger degree than the NIPMAM NG and tends to have a wider temperature range at which this occurs in comparison to the NIPMAM NGs. Similar

trends or behaviour has been noted in other studies for variance in hydrodynamic diameter of NIPAM NG that were compared ([4]). The reason for inconclusiveness from these results as validation of inclusion is one, that the increase is not substantial and small enough to be due to errors or inaccuracy, and two, the molar ratio of CD to NIPMAM is likely a maximum of 1:128 which may not cause a noticeable increase in the critical energy threshold and therefore VPTT. While these results may have been indicative of modification of the NG complex with CD, they alone were inconclusive as they could be explained by a lack of CD in the NG complex or a lack of ability to identify a change due to the large difference in molar ratio. Further testing and validation were attempted with HNMR and FTIR to attempt to verify CD's inclusion.

4.2 HNMR and FTIR – 1st and 2nd Characterisation

The primary characterisation technique used, NMR, was inconclusive for identification of the functionalisation of AACD as well as the inclusion of CD-*co*-NIPMAM NG complex. Issues were encountered with appearance of the characteristic peaks in both AACD, CD-*co*-NIPMAM NG and AA-NIPAM-co-CD NG analyses. These may have related to proton exchange with the solvent, solubility issues of the AACD derivatives of which the distribution was unknown (and therefore hydrophobicity of each derivative being tested), solubility of the NG complexes as well as the problems related to potential presence of water within the DMSO solvent method when preparing the sample. Similar issues were encountered in the testing of the AA coupled NG variation provided from another member in our thesis subgroup. Similar issues with HNMR were encountered for their NIPAM NG's. This method was repeated multiple times with varying concentrations and multiple solvents. However, no viable results were obtained. The method was determined not to be the optimal choice for analysis and focus was shifted to the secondary characterisation technique, FTIR, forgoing the advantage of quantitative analysis of the resulting spectral overlays. NMR results were excluded from analysis of the AACD and NG complexes. Therefore, validation of CD inclusion and DLS results by this technique as well as the molar contributions of NIPMAM vs CD were not obtained or verified.

FTIR in Figure 18 showed the successful functionalisation of Ha-β-CD to AA-CD with the presence of C=O (1679 cm^{-1}), C=C(1640 cm^{-1}) and C-N (1240 cm^{-1}) frequencies appearing in the AA-CD spectrum. C=O (1679 cm^{-1}) would be representative of the highly characteristic amide band expected to be present after the modification of Ha-β-CD. In refinement of the protocol non-amine and non-carboxylate buffer, MES, was used as a more appropriate buffer for the EDC/NHS reaction as it has positive influence overall efficiency of the reaction and due to its non-interference with cross-linking reactions([28]). In later, synthesis steps the AACD derived from the AA-NHS reaction was used as it mitigated a step that may cause further variability in efficiency. This provided confirmation of successful modification of Ha-β-CD in preparation for use as a co-monomer for precipitation polymerisation with NIPMAM. However, this did not provide information on what the degree of functionalisation of AA-CD was present nor information on the mass distribution of functionalised components seen in Figure 7. The efficacy of functionalisation and distribution would have important effects on the crosslinker density, rigidity and encapsulation and release characteristics of the NG. To understand the efficacy of the acrylate functionalisation reaction as well as the distribution of individual variants a **Error! Reference source not found.** was performed on the AA-CD product by Zernike Campus chemistry department post-purification in an acetone ice bath.

Figure 19 illustrated the spectral overlay of AACD, the NIPMAM NG and CD-*co*-NIPMAM NG showing near identical characteristic patterns of absorbance for the NIPMAM and CD-*co*-NIPMAM NG's. The key observation from the FTIR analysis is the absence of the characteristic absorbance pattern of the glucopyranose ring between 700 and 1000cm^{-1} in the CD-*co*-NIPMAM NG. This could be due to accuracy concerns relating to the FTIR technique and the KBr/NG pellets constructed using the milling press, poor transparency, distribution of the NG in the pellets or accuracy of the technique and therefore the sensitivity readings recorded. Numerous attempts were needed to obtain satisfactory spectral data. However, it is hypothesised to likely be due to either the lack of successful inclusion of CD within the target NG complex or intensity issues since the maximum molar equivalence of CD:NIPMAM in the CD-*co*-NIPMAM NG is 1:128 where

the NIPMAM spectrum dominates the reading observed. FTIR as a secondary characterisation step did not verify the inclusion or lack thereof of CD in the target NG.

Comparatively, the FTIR spectral overlay illustrated in Figure 20 showed the presence of the characteristic absorbance pattern of the glucopyranose ring between 700 and 1000cm^{-1}. Although not conclusive on its own, it served as an identification of a potential alternative synthesis method that can successfully incorporate CD into a NIPAM/NIMPMAM NG complex. However, due to its late-stage inclusion no further testing was conducted on the NG complex regarding AZ loading and atypical binding tests. Therefore, its capacity for encapsulation of a hydrophobic drug such as AZ or alternative hydrophobic guest molecules and its efficacy as a nanoscale hydrophobic drug vector are unknown and yet to be tested. Furthermore, due to an error understanding of the protocol a significantly lower molar equivalence of CD was cross-linked with the AA-NIPAM NG resulting in an undesirably low contribution of CD in the NG complex. This has potential limiting implications on the loading capacity of the NG for hydrophobic drug encapsulation and delivery as in the best case only a difference of 0,5% was observed between the base NG and the CD based complex.

4.3 UV/VIS AZ atypical binding and loading

The purpose of the UV/VIS characterisation, loading and triggered release steps were three-fold. First, to determine the loading capacity of the CD-*co*-NIPMAM NG more than any atypical binding that may be expected. Second, to therefore serve as additional verification of the inclusion of CD in the NG complex and successful synthesis. Third, if successful, determine the time-based drug release profile using 365nm light to switch from TRANS to CIS conformation and release the guest molecule. The latter is simultaneously the trigger for the release and activation of the antimicrobial state of the drug developed at Zernike.

The UV/VIS results based procedures described in method sections 2.2.4.2 and 2.2.4.3 showed that AZ retention in the CD-*co*-NIPMAM NG approximately the same as that associated with atypical binding found in the NIPMAM NG. This indicated that AZ 'loaded' in NG was likely only due to entrapment in the NG complex, binding or adhesion to the polymer network itself, regardless of CD or other forms of atypical binding. Both

the CD loading, and the atypical binding results showed approximately 6,6 % binding. During atypical test 2 the precipitate was resuspended between centrifuges showing the lowest atypical binding of 6,08%, 0,5% lower than the CD-co-NIPMAM NG loading test. However, this 0,5% cannot reliably be attributed to hydrophobic loading of the CD cavity due to accuracy of the method, standard deviation of the results in atypical binding and the lack of shift of absorbance peak that would be associated with this type of interaction. It indicated that all the localised AZ in the complex was most likely unrelated the desired hydrophobic bonding with the inner surface of the CD cavity. It is hypothesised that this could be the result of two situations, that there was a lack of access or preference to hydrophobic interaction with the CD cavity or that CD was not successfully copolymerized into the NG complex to begin with. The lack of access could be due to a combination of the degree of cross-linking achieved with AACD functionalisation as well as the significantly low molar contribution of CD within the NG complex. This could lead to atypical interactions outweighing preferential interaction with the inner surface of the CD cavity and therefore to successful entrapment or a lack of sufficient space for the compound to reach the CD. However, this hypothesis is met with caution, as investigations have seen the successful inclusion of hydrophobic compounds in CD derivatives using other polymers and the successful cleavage using enzymes ([5]) in cross-linked polymer-based networks. The hypothesis that there is no CD within the complex can be fortified by some results, such as the FTIR absence of characteristic absorbance patterns but not necessarily by those shown in DLS and VPTT measurements. Further validation and testing would be required for a conclusive answer, some of which have been suggested in Clinical Relevance, Limitations and Recommendations. It was determined that it was not suitable to continue.

4.4 Clinical Relevance, Limitations and Recommendations

The aim of the thesis was to attempt to synthesise and characterise a novel CD based nanogel delivery platform for hydrophobic drug delivery within the human body. The specific initial target was to create a delivery platform for a hydrophobic, AZ-based antimicrobial drug developed at Zernike, Groningen. The focus was to systematically synthesise a novel CD Nanogel, encapsulate and protect the photosensitive hydrophobic molecule modelled as the drug in question and finally investigate its triggered release by irradiation with 365nm light. The triggered release inducing a conformational change from TRANS to CIS states would serve as both the triggered release as well as its activation of its antimicrobial properties. Furthermore, the photosensitive antimicrobial in question would thermally revert to its inactive state over the course of a few hours within the body resulting in no antimicrobial build up or resistance concerns. The clinical relevance, if successful, of such a hydrophobic drug vector would provide a plethora of potential applications and further investigations for various hydrophobic target guest compounds. This could in essence extend as far as investigations into GBM applications such as TMZ as a target hydrophobic drug with the acrylate modification of curcumin to replace BIS as a crosslinker in synthesis.

However, issues were encountered in validation and characterisation steps within the investigation. Successful HNMR was not achieved and had to be excluded as a primary characterisation technique. This in turn limited the ability to verify the functionalisation of the CD for polymerisation suitability as well as the presence of the CD and its glucopyranose ring structures in the target NG. Furthermore, this stifled the ability to determine average molar ratios of the constituents of the NG or functional groups of the AACD compound by comparative peak analysis. Potential solvents discussed at the end of the investigation could be attempted in follow ups as HNMR analysis was not optional due to time constraints and machine failures in closing weeks of the investigation. In further retesting of the suggested series of CD based NG complex at varied molar equivalence, the solvent suggested in HPLC discussion could be attempted. HNMR could be reattempted with a MiliQ diluted acetonitrile solution. This could provide an alternative successful protocol for HNMR. Furthermore, issues could have arisen from the incorrect implementation of this technique, issues with finding suitable

dissolving or the presence of water during preparation using DMSO. Further repetitions should be completed using the above-mentioned solvents as experimental errors may have been the cause of the lack of success. These could be done post inclusion verification from other methods such as the fluorescence technique mentioned in the List of Appendices, page 74.

Further issues were encountered with the secondary characterisation technique, FTIR. While verification was achieved for the conversion of Ha-β-CD to AA-CD, this provided a non-qualitative analysis limiting the information gathered on the degree or efficiency of conversion and therefore degree of crosslinking capability of AACD used as a co-monomer. Moreover, FTIR of the CD-*co*-NIPMAM NG was inconclusive and didn't provide clarity on whether the issue was the technique, the low molar equivalence, or the lack of successful inclusion of CD. Additionally, VPTT measurements didn't show significant enough increases from NIPMAM to CD-*co*-NIPMAM NG to attribute to potential inclusion of CD. It was inconclusive as to whether this was because of low molar contributions in the NG or because of an absence of CD. Therefore, without these validations it could not be substantiated that the substantial increase in average particle diameter was due to successful inclusion of the target compound.

The investigation was unable to test and analyse the loading and release of AZ successfully because of the aforementioned shortfalls in synthesis and verification of CD inclusion in the NG complex. Although these results were less than desirable, they do not mitigate the potential of copolymerisation of CD and NIPMAM for NG synthesis of the hydrophobic drug vector. These results provided the necessary information for the proceeding recommendations for adjustments to protocol and testing in follow up investigations.

With additional time, the investigations could be continued with adjustments to the synthesis protocol and the inclusion of a secondary NIPAM based NG. The first point of order would be to create a series of CD-*co*-NIPMAM NG of varied compositions to verify causes of issues mentioned previously in VPTT, HNMR, FTIR and loading. Molar ratios of 1:5, 1:10 , 1:20, 1:30 and 1:50 of CD:NIPMAM could be created using the protocols illustrated in Figure 10 with functionalisation of CD following the more efficient protocol depicted in Figure 6.

These results could be cross-referenced to verify whether the increase in the average hydrodynamic diameter seen in the DLS is the result of inclusion of CD in the NG complex or resulting from confounding variables in the NG structure or measurements. Furthermore, even if HNMR is unsuitable, higher molar contributions of CD could potentially solve FTIR intensity issues related to the appearance of the characteristic absorbance pattern for the glucopyranose ring structure from the CD in the CD-*co*-NIPMAM NG. This could provide further validation of CD inclusion. Alternatively, or in conjunction with this Nile Red fluorescence could be used to verify the inclusion of CD prior to further characterisation or AZ loading tests. The method of which is described in the List of Appendices, page 74.

The series of 5 CD-*co*-NIPMAM NG's azo benzene loading using centrifugation or preferably the slower dialysis method could be used to determine if the low molar equivalence of CD in the NG complex was a key load limiting factor for AZ. If the relative contribution of hydrophobic encapsulation vs atypical binding was lost in the inaccuracy of the DLS technique for a 128:1 ratio this would become increasingly apparent among the 5 NG's. A more definitive loading capacity could be determined for the target NG. Should these results prove more successful the AZ triggered release test mentioned in section 3.4.2 could be tested on each to determine a triggered release profile and if any variation occurs based on the morphological variance.

The HPLC-MS results of the acrylate functionalisation could be used to identify the relative distribution and isolate specifically functionalised units. This could be useful if a desirable rigidity or degree of cross-linker was applicable for Zernike or other applications of hydrophobic drug encapsulation or shrinking and swelling behaviour were desired. However, this would depend on the specific yields of each compound and, therefore, on the relative ease and cost of obtaining specifically functionalised comonomers.

This derivative production information could be of significant values. Other studies have looked at CD derivatives and their relative reactivity in polymerisation. These results have indicated variance is affinity to co-polymerise or co-precipitate based on the level and type of functionalisation achieved ([8]). Information on the distribution could provide

valuable insight into why the achieved distribution, without derivative isolation, may have impacted the apparent success of synthesis.

Lastly, the NIPAM NG created by Irem Soyhan could be re-synthesised and coupled with CD using the method described in the List of Appendices, page 73. If VPTT being below 37°C is not of critical importance, the above-mentioned investigations could be conducted on varied CD molar ratios using the NIPAM NG.

In summary, success was achieved for the inclusion of CD within a NIPAM/NIPMAM based NG complex fulfilling one of the main objectives of this investigation. Furthermore, drug modelling and characterisation of this Nanogel could provide valuable insight into its practical or clinical potential. Additionally, the primary synthesis method could be adjusted and retested to potentially verify its success. This would provide an alternative and potentially simpler method of achieving the aim, synthesising a CD based nanoscale drug delivery platform. Having two successful synthesis protocols using two different thermosensitive polymers would allow for variability of NG construction depending on the specific use intended. While some experimental procedures did not produce desirable results, there were indications that the method has the potential for success if investigated further. Functionalisation of the CD was successful and further useful information on this specific process could obtained. HPLC results would also provide information on the efficacy of functionalisation. With this information on the distribution, specific variations could be isolated. With isolation, cost-effectiveness of specific derivatives could be estimated as well as providing the opportunity to fine tune the cross-linker density and their rigidity of the complex. These could have implications on drug loading and entrapment control for future synthesis. Additionally, important information was obtained on the specific atypical binding that can be expected with these NG complex's regardless of the inclusion of CD. Further testing could provide information on what mechanism of release is required for the atypically bound drug molecules and how this may impact the nanogel behaviour.

5 Conclusions

The aim of the research was to synthesise a novel CD-based nanogel delivery platform for hydrophobic drug delivery. The focus of the investigation was to create this novel nanogel for the primary purpose of encapsulating a photosensitive enantiomer based antimicrobial drug developed in the past few years at Zernike Campus. An antimicrobial with significant clinical potential and the ability to self-regulate deactivation within the body. This was attempted using a clinically relevant and simple co-precipitation polymerisation technique utilising NIPMAM and a functionalised derivative of a β-CD, which are known to have synergetic properties with various nanoscale drug delivery vectors and applications.

Difficulties were experienced in characterisation and successful loading and encapsulation. While potentially successful in synthesis, the inconclusive results of characterisation and loading require further testing of the NG. Various molar compositions of CD should be characterised to make conclusive determinations on loading capacity and triggered release profiles for use as a hydrophobic drug vector. Characterisation techniques were not sufficient for verification of the NG's properties. Loading tests were not dissimilar enough from atypical binding expectations to make conclusive estimations of the CD cavities capacity potential. Triggered release testing and profiling were not achieved for the NG complex because of this. This investigation was not conclusively successful in developing a CD-based nanogel platform for hydrophobic drug delivery or specifically the delivery of the AZ based antimicrobial developed at Zernike. Further investigations should be carried out at varied molar compositions of the CD-*co*-NIPMAM NG complex to provide reliable characterisation, clinical and practical potential and verify the success and efficiency of the proposed synthesis approach.

Important success was achieved in one synthesis method, using NIPAM, that could be followed be further testing and validation as a drug vector. CD was successfully functionalised, and HPLC-MS data would provide important insight into efficiency and derivative selection nanogel rigidity, encapsulation, and entrapment. These derivatives could be isolated for other purposes outside the aims of this investigation as CD has a

wide range of applications. Important information was gathered regarding the atypical binding affinity of the base NIPMAM NG complex and could be further tested for analysing its impact on loading and NG behaviour. Potential success could be verified for the simpler primary synthesis technique with further protocol adjustments and retesting, providing a second method of synthesis using NIPMAM instead of NIPAM for specific intended uses.

6 Ethics Paragraph

The only key ethical questions topics relevant to this thesis topic would concern extensions of this investigation but not the investigation itself. These would relate to the use of nanoparticles and UV triggered release mechanisms and their potential impact on human health, healthy human tissue and potential cytotoxicity related to implementing modified nanoparticulate treatments for drug delivery ([7,33]). However, CD based derivatives have been proven not only to be synergetic in inclusion with clinical prominent polymers but have shown successful clinical relevance for nanoscale drug delivery systems ([15]). Nanoparticles concerns that relate cytotoxicity usually entail the use of modification with compounds such as silver, gold or "combination products" that are essentially nanoparticles encapsulating chemotherapy components and need to go through approval before studies are conducted on animal or human tissue or relating to in vitro investigations ([20]). Most of the significant ethical issues that surround nanomedicine in general relate to risk assessment, risk management and risk communication in clinical trials and associated investigations in these areas ([21]).

I would argue that this investigation does not breach on any ethical concerns related to the actual application of antimicrobials, chemotherapy drugs or any other hydrophobic drug related treatments. Although the conclusions and results of this investigation could be carried out further in some areas of nanoparticle synthesis for these purposes, no actual drugs were used, in vitro or in vivo studies were conducted. No tests were conducted concerning antimicrobial effectiveness, no antimicrobial or chemotherapy drug were utilised, no pilot studies, proposals for pilots or cultures were used in the testing. The investigation simply looked at synthesis or characterisation of this nanogel delivery platform. All extensive testing that would relate to specific drug or antimicrobial uses have been carried out by the researchers from which the motivation has been drawn for the AZ based antimicrobial drug. The ethical responsibility and onus of cytotoxicity, safety limitations of use and implementation of the nanoparticle and encapsulated drugs as well as considerations for safe use of UV/VIS based irradiation ([7,33]) for triggered release falls on those responsibility for carrying out further

investigations of this research project. Any ethical and moral considerations would align with their investigative questions and assessments.

The potential societal impact of this research, successful or not, is the generation of a contribution towards antimicrobial, photo-pharmacological, chemotherapy and general hydrophobic drug intervention treatments in biomedical engineering. Contributions to these areas of healthcare could have significant potential social impacts on effective treatment alternatives and mitigate concerns about antimicrobial build-up. These could have significant impacts on current health crises across the world ([24,29,33]). However, while having potential implications, this investigation does not include extensive integration, use or in vitro testing and therefore hold less ethical obligation than follow up studies may encounter.

Lastly from an ethical stance all information should presented as it is, failures, limitations and errors clearly identified. Furthermore, it is essential to cite and reference all sources of literature or contributions made to the thesis in a standard and acceptable format. All information gathered in this research investigation is essentially property of the Biomedical Engineering Department of UMCG, under the research group of Patrick van Rijn and will remain confidential and not be shared or made public knowledge without the consent of the department or group or unless made publicly available by either party.

List of Literature

1. Alphandéry E. Nano-Therapies for Glioblastoma Treatment. *Cancers 2020, Vol 12, Page 242*. 2020;12(1):242. doi:10.3390/CANCERS12010242
2. Angelini G, Campestre C, Scotti L, Gasbarri C. molecules Kinetics and Energetics of Thermal Cis-Trans Isomerization of a Resonance-Activated Azobenzene in BMIM-Based Ionic Liquids for PF 6 − /Tf 2 N − Comparison. Published online 2017. doi:10.3390/molecules22081273
3. Bandyopadhyay S, Sharma A, Ashfaq Alvi MA, Raju R, Glomm WR. A robust method to calculate the volume phase transition temperature (VPTT) for hydrogels and hybrids. *RSC Advances*. 2017;7(84):53192-53202. doi:10.1039/C7RA10258E
4. Bucatariu S, Fundueanu G, Prisacaru I, et al. Synthesis and characterization of thermosensitive poly(N-isopropylacrylamide-co-hydroxyethylacrylamide) microgels as potential carriers for drug delivery. *Journal of Polymer Research*. 2014;21(11). doi:10.1007/S10965-014-0580-7
5. Chen J, Garcia ES, Zimmerman SC. Intramolecularly Cross-Linked Polymers: From Structure to Function with Applications as Artificial Antibodies and Artificial Enzymes. *Accounts of Chemical Research*. 2020;53(6):1244-1256. doi:10.1021/ACS.ACCOUNTS.0C00178
6. Duracher D, Elaïssari A, Pichot C. Characterization of cross-linked poly(N-isopropylmethacrylamide) microgel latexes. *Colloid and Polymer Science*. 1999;277(10):905-913. doi:10.1007/S003960050470
7. Fatima F, Siddiqui S, Khan WA. Nanoparticles as Novel Emerging Therapeutic Antibacterial Agents in the Antibiotics Resistant Era. *Biological Trace Element Research 2020 199:7*. 2020;199(7):2552-2564. doi:10.1007/S12011-020-02394-3
8. Glöckner P, Schollmeyer D, Ritter H. X-ray diffraction analysis of butyl- and isobornyl acrylate/heptakis(2,6-di-O-methyl)-β-cyclodextrin complexes and correlation to 1H NMR-spectra. *http://dx.doi.org/101163/156855502760157890*. 2012;5(2-3):163-172. doi:10.1163/156855502760157890
9. Haimhoffer Á, Rusznyák Á, Réti-Nagy K, et al. Cyclodextrins in drug delivery systems and their effects on biological barriers. *Scientia Pharmaceutica*. 2019;87(4). doi:10.3390/SCIPHARM87040033
10. Ikhimiukor OO, Odih EE, Donado-Godoy P, Okeke IN. A bottom-up view of antimicrobial resistance transmission in developing countries. *Nature Microbiology 2022 7:6*. 2022;7(6):757-765. doi:10.1038/s41564-022-01124-w
11. Keskin D, Mergel O, van der Mei HC, Busscher HJ, van Rijn P. Inhibiting Bacterial Adhesion by Mechanically Modulated Microgel Coatings. *Biomacromolecules*. 2019;20(1):243-253. doi:10.1021/ACS.BIOMAC.8B01378/ASSET/IMAGES/LARGE/BM-2018-01378G_0007.JPEG
12. Keskin D, Zu G, Forson AM, Tromp L, Sjollema J, van Rijn P. Nanogels: A novel approach in antimicrobial delivery systems and antimicrobial coatings. *Bioactive Materials*. 2021;6(10):3634-3657. doi:10.1016/J.BIOACTMAT.2021.03.004

13. Kono H, Teshirogi T. Cyclodextrin-grafted chitosan hydrogels for controlled drug delivery. *International Journal of Biological Macromolecules*. 2015;72:299-308. doi:10.1016/J.IJBIOMAC.2014.08.030
14. Łagiewka J, Girek T, Ciesielski W. Cyclodextrins-peptides/proteins conjugates: Synthesis, properties and applications. *Polymers (Basel)*. 2021;13(11). doi:10.3390/POLYM13111759
15. Lee JU, Lee SS, Lee S, Oh H bin. Noncovalent complexes of cyclodextrin with small organic molecules: Applications and insights into host–guest interactions in the gas phase and condensed phase. *Molecules*. 2020;25(18). doi:10.3390/MOLECULES25184048
16. Lee NY, Ko WC, Hsueh PR. Nanoparticles in the treatment of infections caused by multidrug-resistant organisms. *Frontiers in Pharmacology*. 2019;10:1153. doi:10.3389/FPHAR.2019.01153/BIBTEX
17. Mauri E, Giannitelli SM, Trombetta M, Rainer A. Synthesis of nanogels: Current trends and future outlook. *Gels*. 2021;7(2). doi:10.3390/GELS7020036
18. Moya-Ortega MD, Alvarez-Lorenzo C, Sigurdsson HH, Concheiro A, Loftsson T. Cross-linked hydroxypropyl-β-cyclodextrin and γ-cyclodextrin nanogels for drug delivery: Physicochemical and loading/release properties. *Carbohydrate Polymers*. 2012;87(3):2344-2351. doi:10.1016/J.CARBPOL.2011.11.005
19. Plamper FA, Richtering W. Functional Microgels and Microgel Systems. *Accounts of Chemical Research*. 2017;50(2):131-140. doi:10.1021/ACS.ACCOUNTS.6B00544
20. Resnik DB, Tinkle SS. Ethical Issues in Clinical Trials Involving Nanomedicine. *Contemp Clin Trials*. 2007;28(4):433. doi:10.1016/J.CCT.2006.11.001
21. Resnik DB, Tinkle SS. Ethics in Nanomedicine. *Nanomedicine (Lond)*. 2007;2(3):345. doi:10.2217/17435889.2.3.345
22. Richtering W, Alberg I, Zentel R, Richtering W, Alberg I, Zentel R. Nanoparticles in the Biological Context: Surface Morphology and Protein Corona Formation. *Small*. 2020;16(39):2002162. doi:10.1002/SMLL.202002162
23. Ryu JH, Chacko RT, Jiwpanich S, Bickerton S, Babu RP, Thayumanavan S. Self-cross-linked polymer nanogels: A versatile nanoscopic drug delivery platform. *J Am Chem Soc*. 2010;132(48):17227-17235. doi:10.1021/JA1069932
24. Sharmin S, Rahaman MM, Sarkar C, Atolani O, Islam MT, Adeyemi OS. Nanoparticles as antimicrobial and antiviral agents: A literature-based perspective study. *Heliyon*. 2021;7(3):e06456. doi:10.1016/J.HELIYON.2021.E06456
25. Simeth NA, Kinateder T, Rajendran C, et al. Towards Photochromic Azobenzene-Based Inhibitors for Tryptophan Synthase. *Chemistry - A European Journal*. 2021;27(7):2439-2451. doi:10.1002/CHEM.202004061
26. Szente L, Singhal A, Domokos A, Song B. molecules Cyclodextrins: Assessing the Impact of Cavity Size, Occupancy, and Substitutions on Cytotoxicity and Cholesterol Homeostasis. Published online 2018. doi:10.3390/molecules23051228
27. Takeshita T, Hara M. Photoionization and trans-to-cis isomerization of β-cyclodextrin-encapsulated azobenzene induced by two-color two-laser-pulse excitation. *Spectrochimica Acta Part A: Molecular and Biomolecular Spectroscopy*. 2018;193:475-479. doi:10.1016/J.SAA.2017.12.061

28. Vashist SK. Comparison of 1-Ethyl-3-(3-Dimethylaminopropyl) Carbodiimide Based Strategies to Crosslink Antibodies on Amine-Functionalized Platforms for Immunodiagnostic Applications. *Diagnostics*. 2012;2(3):23-33. doi:10.3390/DIAGNOSTICS2030023
29. Velema WA, van der Berg JP, Hansen MJ, Szymanski W, Driessen AJM, Feringa BL. Optical control of antibacterial activity. *Nature Chemistry*. 2013;5(11):924-928. doi:10.1038/nchem.1750
30. Wagner-Wysiecka E, Łukasik N, Biernat JF, Luboch E. Azo group(s) in selected macrocyclic compounds. *Journal of Inclusion Phenomena and Macrocyclic Chemistry 2018 90:3*. 2018;90(3):189-257. doi:10.1007/S10847-017-0779-4
31. Wang L, Hu C, Shao L. The antimicrobial activity of nanoparticles: present situation and prospects for the future. *International Journal of Nanomedicine*. 2017;12:1227. doi:10.2147/IJN.S121956
32. Wankar J, Kotla NG, Gera S, Rasala S, Pandit A, Rochev YA. Recent Advances in Host–Guest Self-Assembled Cyclodextrin Carriers: Implications for Responsive Drug Delivery and Biomedical Engineering. *Advanced Functional Materials*. 2020;30(44). doi:10.1002/ADFM.201909049
33. Wegener M, Hansen MJ, Driessen AJM, Szymanski W, Feringa BL. Photocontrol of Antibacterial Activity: Shifting from UV to Red Light Activation. *J Am Chem Soc*. 2017;139(49):17979-17986. doi:10.1021/jacs.7b09281
34. Yi P, Wang Y, He P, et al. Study on β-cyclodextrin-complexed nanogels with improved thermal response for anticancer drug delivery. *Materials Science and Engineering C*. 2017;78:773-779. doi:10.1016/J.MSEC.2017.04.096
35. Zhang D, Yang X. Precipitation Polymerization. *Encyclopedia of Polymeric Nanomaterials*. Published online 2014:1-10. doi:10.1007/978-3-642-36199-9_282-1
36. Zu G, Mergel O, Ribovski L, Bron R, Zuhorn IS, van Rijn P. Nanogels with Selective Intracellular Reactivity for Intracellular Tracking and Delivery. *Chemistry - A European Journal*. 2020;26(66):15084-15088. doi:10.1002/CHEM.202001802
37. Zu G, Mergel O, Ribovski L, Bron R, Zuhorn IS, van Rijn P. Nanogels with Selective Intracellular Reactivity for Intracellular Tracking and Delivery. *Chemistry - A European Journal*. 2020;26(66):15084-15088. doi:10.1002/CHEM.202001802
38. Zu G, Steinmüller M, Keskin D, van der Mei HC, Mergel O, van Rijn P. Antimicrobial Nanogels with Nanoinjection Capabilities for Delivery of the Hydrophobic Antibacterial Agent Triclosan. *ACS Applied Polymer Materials*. 2020;2(12):5779-5789. doi:10.1021/ACSAPM.0C01031

List of Appendices

Appendix 1: UV/VIS Calibration Data 66
Appendix 2: UV/VIS Loading Spectra and Atypical tests 68
Appendix 3: Method used for synthesising the NIPAM-co-AA NG and Coupling technique with Ha-β-CD..... 73
Appendix 4: Fluorescence Plate Reader – CD inclusion verification 74

Appendix 1: UV/VIS Calibration Data

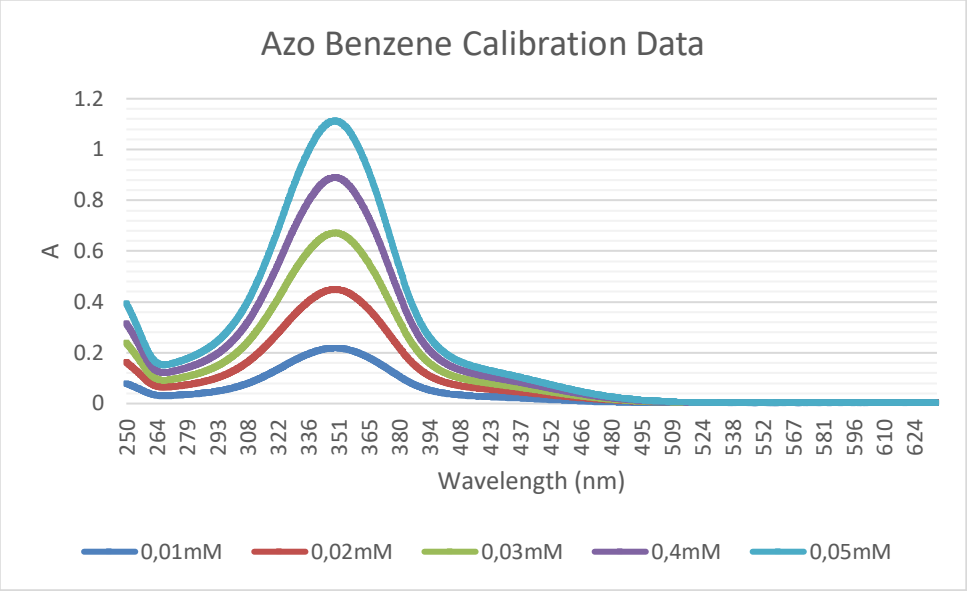

Figure 22 UV/VIS Spectra for various Molarities of Azo Benzene used to construct the standard curve for concentration calibration. Measured wavelength range between 250nm and 700nm using quarts cuvette.

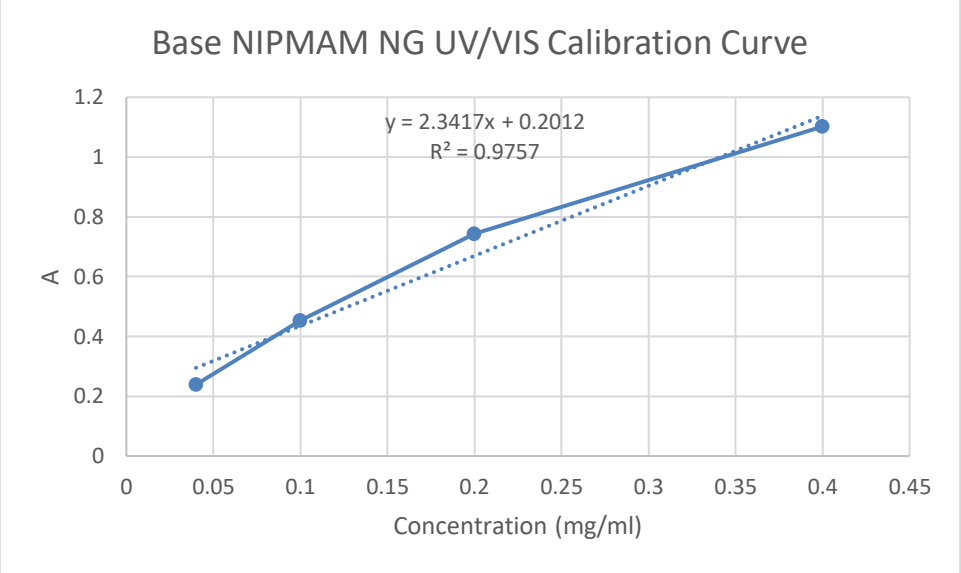

Figure 23 Standard curve for NIPMAM NG constructed in first protocol test for UV/VIS.

Horizontal axis units were left in mg/ml as molecular weight of the nanogel was unknown. The curve was not used in further analysis other than ensuring absorbance contribution was within acceptable S/N ratio limits at the 350nm focal point for AZ absorbance in the atypical binding test.

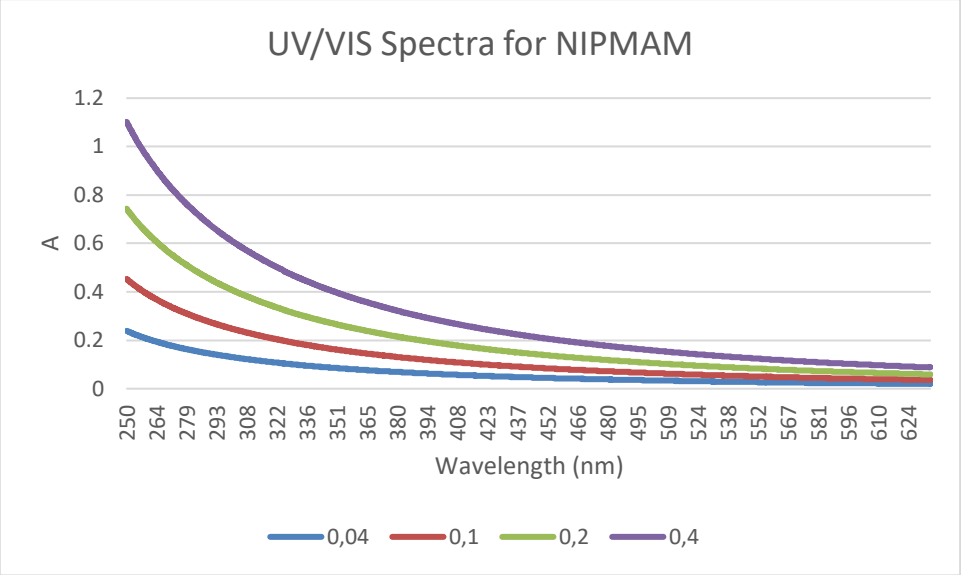

Figure 24 UV/VIS spectra of various concentrations of NIPMAM NG. Legends are in in mg/ml as molecular weight is unknown.

Appendix 2: UV/VIS Loading Spectra and Atypical tests

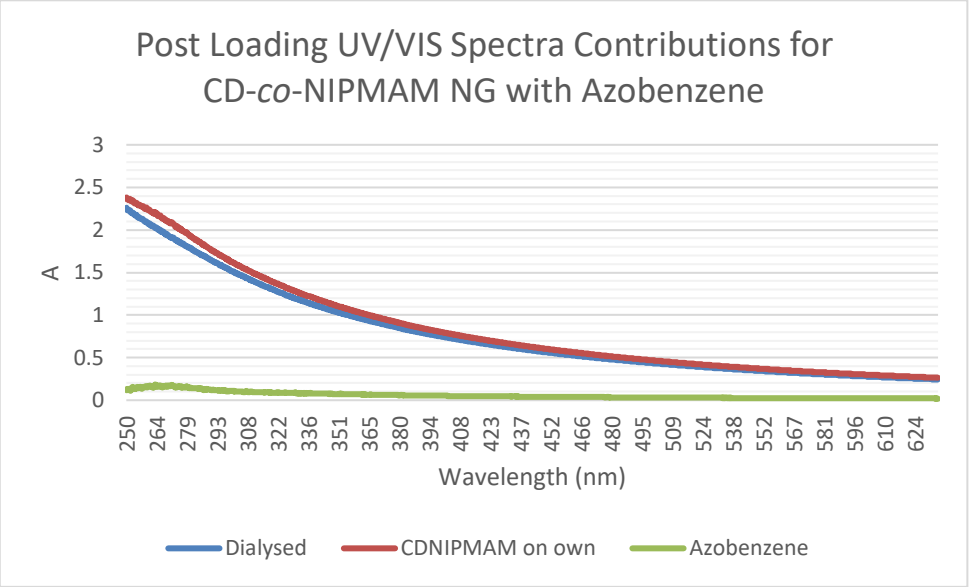

Figure 25 UV/VIS Spectra normalised and original CD NG contribution subtracted to show AZ Molarity in CD-co-NIPMAM NG post dialysis for 5 days in MiliQ.

S/N ratios were above 1 ABS for readings below 350nm. However, reading were only necessary for comparison at 350nm where the expected peak for AZ is located. Concentration of AZ and CD were increased to as close to 1ABS as possible at 350nm in order to maximise the presence of CD in the testing while maintaining an approximate 1:1 molar ratio of AZ to CD in the NG complex. This ratio was approximated based on the assumption that the relative molar contributions in the NG complex were equal to those use in the synthesis procedure which was 128:1 of NIPMAM to AACD. While indicative of an approximate loading the data does not, at this low concentration of AZ, show a significant absorbance peak at 350nm as would be expected with the presence of AZ.

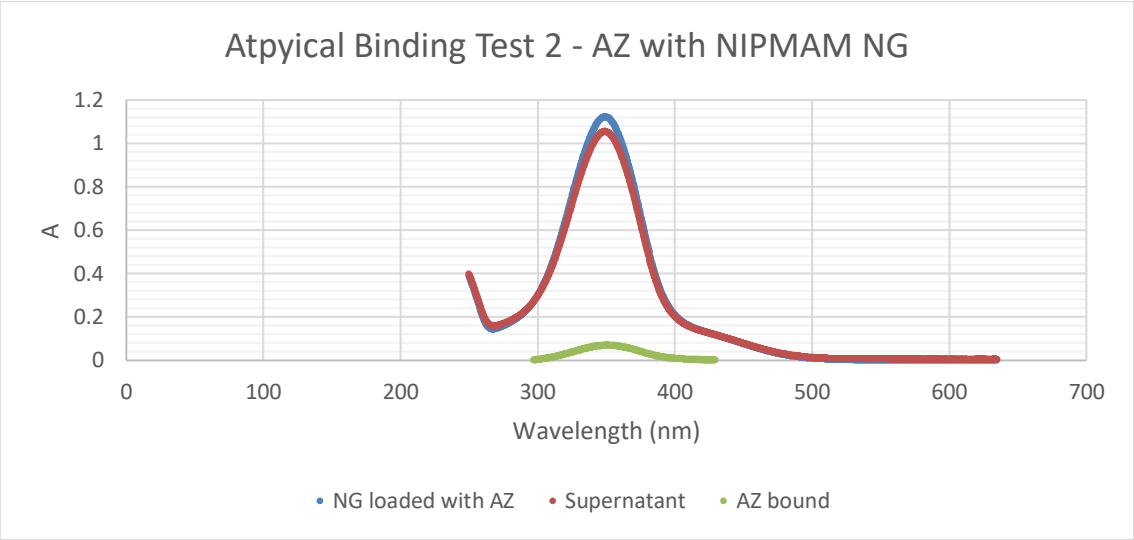

Figure 26 Resulting Spectral overlay of atypical test 2 with NIPMAM NG and AZ. Solution was incubated for 2 days and centrifuged four times at 16 000 RPM (38 400 rcf) for 1 hour.

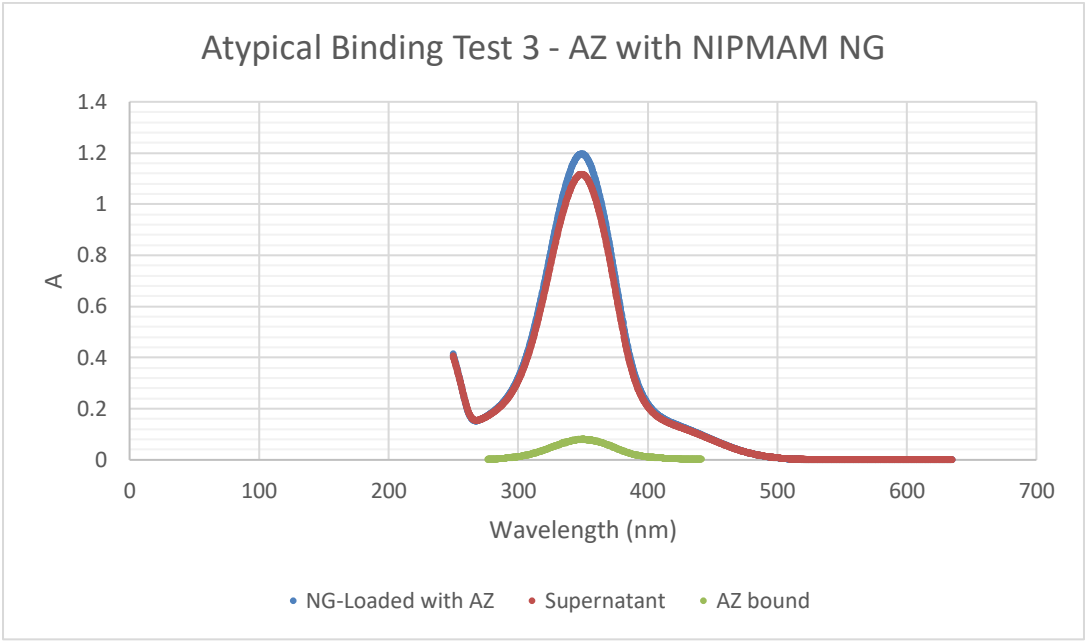

Figure 27 Resulting Spectral overlay of atypical test 3 with NIPMAM NG and AZ. Solution was incubated for 2 days and centrifuged four times at 16 000 RPM (38 400 rcf) for 1 hour.

Spectral overlay of the Atypical binding test was not available for Test 1 as the supernatant absorbance list file was corrupt and only the peak data was available for use in the atypical binding approximation. The Atypical binding test 2 was the test that had the lowest S/N ratio and was resuspended in between each centrifuge of 1 hr to ensure detachment of loosely bound AZ. Atypical test 2 was considered the most reliable of the three tests.

Table 4 Results of Atypical test 1,2 and 3 for AZ with the NIPMAM NG

Atypical test 1

	Wavelength of Peak (nm)	Absorbance	mM	Atypical Binding %
Azo Benzene loaded	349,4	1,13	0,051	6,99
Supernatant Measurement	349,2	1,05	0,004	

Atypical Test 2

	Wavelength of Peak (nm)	Absorbance	mM	Atypical Binding %
Azo Benzene loaded	349,2	1,12	0,053	6,08
Supernatant Measurement	349,2	1,05	0,050	

Atypical Test 3

	Wavelength of Peak (nm)	Absorbance	mM	Atypical Binding %
Azo Benzene loaded	349,0	1,20	0,057	6,70
Supernatant Measurement	349,0	1,12	0,053	

Average atypical binding was approximated as 6,59±0,46%. The perceived most reliable of these three tests which included resuspension of the precipitate between each centrifuge was atypical test with an atypical binding approximation of 6,08%.

A shift in UV/VIS absorbance peaks that could be expected with a shift from TRANS or CIS conformations of AZ are shown in FIGURE 28 below. This figure was obtained from a publication looking isomerization of a similar compound, methoxy AZ (MeO-AZ). This known shift was used to verify that AZ being loaded in the atypical binding test with the NIPMAM NG and the loading test for CD-*co*-NIPMAM NG were in the required TRANS conformation and not a mixture of TRANS and CIS. This was essential and the CIS conformation was not the conformation needed to form hydrophobic interaction with the CD cavity within the CD-*co*-NIPMAM NG.

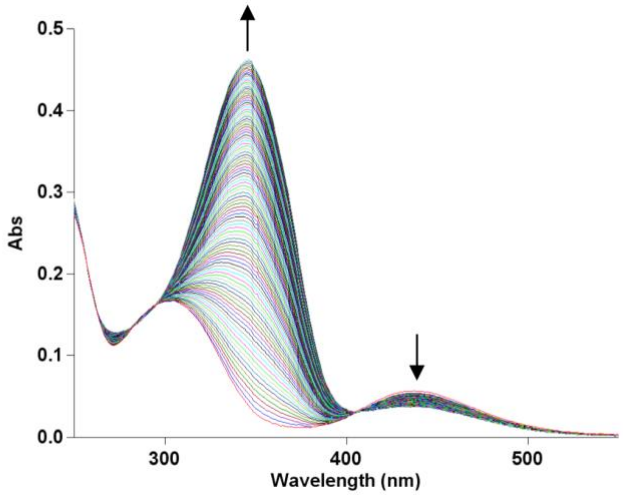

Figure 28 Example UV/VIS CIS-TRANS isomerisation for MeO-AZ in BMIM PF_6 , this illustration was derived from an open source publication([2]).While not the exact AZ used in the experiments mentioned in this investigation the characteristic peak pattern change between Trans (the left arrow peak) and CIS (right arrow peak around 420-430nm) conformations are similar. A similar expected UV/VIS shift was experienced and expected for results relating conformation between TRANS and CIS states of AZ.

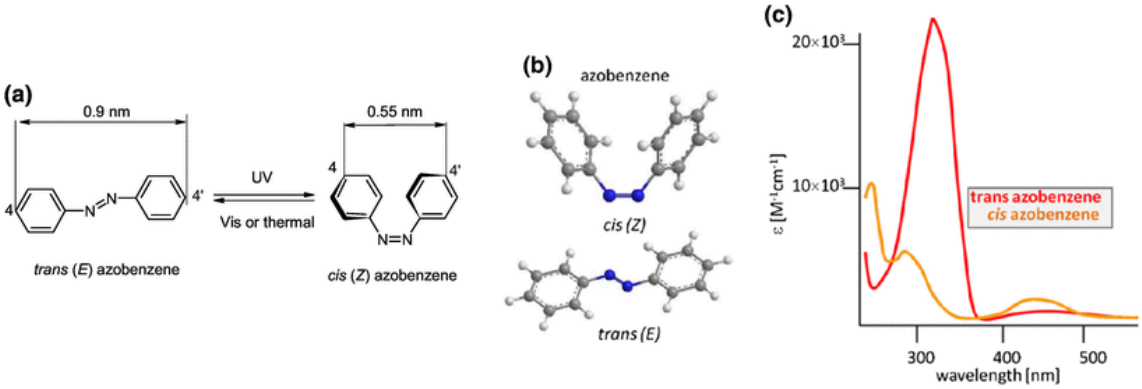

Figure 29 Illustration of AZ TRANS and CIS conformational states and expected variance in characteristic UV/VIS absorbance patterns, this illustration was derived from an open source publication ([30]). These expected variations in characteristic pattern were used to ensure UV/VIS measurements were taken using solutions of purely one conformational state when required for atypical binding or loading tests.

The outcomes of the irradiation protocol would be expected upon initial irradiation time frames to be a mixture of CIS and TRANS conformations. TRANS conformations, the red series in Figure 29, would be expected to be measured prior to irradiation or within the NG complex. CIS absorbance patterns would be expected within the supernatant for the released AZ as this is the thermodynamically unstable conformational state that would no longer retain its hydrophobic interaction with the CD pocket.

Triggered release testing additional points and reflection:

It is known from the protocols for preparing the azobenzene for loading and testing prior to triggered release testing that isolation in a hot bath in the dark showed a characteristic peak at 350nm, characteristic of the TRANS conformation in UV/VIS measurements. No CIS was present in the mixture as no 310-330nm and 420-433nm peaks were observed in UV/VIS measurements. Switching of CIS to TRANS in preparation was successful. An example of the expected shifts in peaks between TRANS and CIS can be found by List of Appendices, page 71. This known characteristic shift between CIS and TRANS in UV/VIS spectra was used to ensure that the AZ was not a mixture of CIS and TRANS conformations and that purely TRANS AZ was being utilised for the atypical binding test with NIPMAM and the loading test with CD-*co*-NIPMAM NG in all UV/VIS experiments. This was essential as the TRANS conformation would be strongly bound by hydrophobic interactions to the hydrophobic face of the CD cavity. The CIS conformation would be weakly bound and released, which is what was desired for triggered release tests and not the loading protocols. The expected results from triggered release testing can be found in the same illustration, Figure 28 and Figure 29. Upon irradiation an expected mixture of CIS and TRANS conformations would be measured in UV/VIS. Upon continued irradiation of light, the peak would towards a higher relative yield of CIS characteristic pattern as the AZ was released during its conformational change from TRANS to CIS. However, a full conversation of TRANS to CIS conformation was not necessary expected as has been pointed out in previous studies ([27]).

Appendix 3: Method used for synthesising the NIPAM-co-AA NG and Coupling technique with Ha-β-CD

NIPAM (12.370 mmol), Acrylic acid (1.887 mmol), BIS (0.214 mmol) and SDS (0.197 mmol) were dissolved in 100 mL distilled water. The mixture was heated to 70 °C and purged with nitrogen for 1 hour. After 1 hour purging the polymerization reaction was initiated with degassed APS solution (0.06M, 5mL). Reaction mixture was stirred for 6 hours at 70 °C under nitrogen stream. After 6 hours heat and nitrogen were shut down and reaction left for overnight with continuous stirring. The formed nanogels were dialysed (12-14 kDA cutoff) for 1 week against distilled water at room temperature.

This methodology was provided by Irem Soyhan from her thesis where she synthesised NIPAM-co-AA nanoparticles. These nanoparticles were provided for an additional synthesis method using EDC/NHS to couple CD to the NIPAM NG.

This NG was coupled with Ha-β-CD to form a CD inclusive NG complex. The method of which follows: 390,48mg of MES was added to 20ml MiliQ and the pH was adjusted to 6 with 5M NaOH. 10mg of AAc-NIPAM NG , 62,3mg of EDC and 37,4mg of NHS was added to the MES buffer solution and left to stir in the dark for 2hours. The pH was then adjusted to 7,72 (should be between 7 and 8) by adding 5M NaOH. 20mg of Ha-β-CD was then added gently to allow it to dissolve and was left stirring overnight. The solution was then dialysed against MiliQ for 3-7 days using 6-8kDa MWCO tubing. The MiliQ was refreshed 3 times a day. The resulting solution was freeze dried overnight at -40℃ for 24 hours.

Appendix 4: Fluorescence Plate Reader – CD inclusion verification

A further validation test was conducted for the inclusion of CD in the AA-CD-*co*-NIPMAM NG, in addition to FTIR and HNMR. For this a fluorescence spectrum analysis was conducted using Nile Red fluorescent dye and the Synergy H1 Mircoplate reader. Four sample solutions were creating where Nile Red was incubated for 2 days with the following compounds: β-CD, plain MiliQ, NIPMAM NG and the AA-CD-*co*-NIPMAM NG. 1:1 molar ratio was used for β-CD: Nile Red, NIPMAM NG: Nile Red and AA-CD-*co*-NIPMAM NG: Nile Red as well as MiliQ. The mixed solutions were then placed in dialysis tubing to dialyse vs 96% EtOH for 3 days with EtOH refreshing twice a day to dissolve the excess Nile Red. These solutions were then re-dialysed for 5 days in MiliQ with refreshment twice a day. The solutions were then freeze dried overnight and the samples were then suspended in fresh MiliQ for further analysis with the plate reader. The MiliQ and β-CD samples were used as controls for comparison of fluorescence intensity observed in the spectral analysis of NIPMAM NG: and AA-CD-*co*-NIPMAM. No quantitative analysis was conducted, and a full spectrum analysis was measured for the purpose of observing fluorescence intensity shifts and changes to that could be attributed to the inclusion CD in the co-polymerised NG and serve as verification. The four samples were added to a 96 well plate, uncovered. These four samples were then measured with full spectrum analysis with excitation wavelength of 552nm and emission spectral range of 550nm to 700nm. The spectra were graphed together, and comparisons made between the controls and the two nanogels.